Angle Rigidity for Multiagent Formations in 3-D

Liangming Chen and Ming Cao, *Fellow, IEEE*

***Abstract*—This article establishes the notion and properties of angle rigidity for 3-D multipoint frameworks with angle constraints, and then designs direction-only control laws to stabilize angle rigid formations of mobile agents in 3-D. Angles are defined using the interior angles of triangles within the given framework, which are independent of the choice of coordinate frames and can be conveniently measured using monocular cameras and direction-finding arrays. We show that 3-D angle rigidity is a local property, which is in contrast to the 3-D bearing rigidity as has been proved to be a global property in the literature. We demonstrate that such angle rigid and globally angle rigid frameworks can be constructed through adding repeatedly new points to the original small angle rigid framework with carefully chosen angle constraints. We also investigate how to merge two 3-D angle rigid frameworks by connecting three points of one angle rigid framework simultaneously to the other. When angle constraints are given only in the surface of a framework, angle rigidity of convex polyhedra is studied, in which the cases of triangular face and triangulated face are considered, respectively. The proposed 3-D angle rigidity theory is then utilized to design decentralized formation control strategies using local direction measurements for teams of mobile agents. Simulation examples are provided to validate the convergence of the formations.**

***Index Terms*—3-D angle rigidity, angularity, direction/angle measurements, formation control, multiagent systems.**

I. Introduction

RIGIDITY of multipoint frameworks has been extensively studied for centuries as a mathematical topic in graph theory [1], [2], which has also been used as an insightful notion in many application scenarios, e.g., multiagent formations [3], material structures [4], and biological tissues [5]. Rigidity theory has primarily been used to characterize the stiffness of a framework with distance constraints for the discussion of distance rigidity [6]. When such constraints are properly chosen, the multipoint framework can be locally (resp. globally) rigid if all the interpoint distances are constant under local (resp. global) perturbations; otherwise, the framework is said to be nonrigid or flexible [7]. Therefore, how to select distance constraints to construct distance rigid frameworks and how to check a framework's distance rigidity constitute the main subjects of distance rigidity theory [6]. However, those construction and checking conditions depend on the dimension d of the space where those vertices are embedded. For example, for generic frameworks, Hendrickson has conjectured that if a graph $\mathcal{G}$ is $(d+1)$-connected and redundantly rigid (the definition of redundant rigidity can be found in [7, Sect. 1.2]), then $\mathcal{G}$ is globally rigid, which has later been proved to be true for $d = 1, 2$ [8] but false for $d \geq 3$ [9]. Recently, bearing rigidity has been studied for frameworks with bearing constraints [10], [11], [12]. According to [10], when bearing constraints are given in coordinate frames with the same orientation, local bearing rigidity implies global bearing rigidity for an arbitrary dimension d. Without relying on the alignment of coordinate frames, angle rigidity has been studied recently for 2-D frameworks [13], [14] and d-dimensional frameworks [15], respectively. However, even when angle constraints are defined with a specific direction in 2-D [14], it has been shown that the resulting angle rigidity is a local property since angle rigidity does not imply global angle rigidity. Although 2-D angle rigidity [13], [14] and algebraic checking conditions for d-dimensional angle-constrained frameworks have been developed [15], angle rigidity in 3-D is more complicated and its main properties, such as construction methods, have not been adequately studied.

In addition to the theoretical significance, rigidity theory plays an important role in the application of multiagent formations [3], [16], [17], [18]. Using distance rigidity, formation control laws have been proposed for a team of mobile agents with relative position measurements in their local coordinate frames [19], [20], [21]. To make full use of low-cost and lightweight onboard sensors, e.g., monocular cameras and sensor arrays [22], using bearing rigidity theory, a bearing-only formation law has been designed [10] for a group of agents with aligned coordinate frames. Without the requirement on the alignment of agents' coordinate frames, angle/direction-based formation control algorithms have been proposed using angle rigidity [13], [14] or infinitesimal shape-similarity [15]. For the direction-only formation approaches proposed in [14], no communication and distance measurements among the agents are needed. However, the direction-only formation algorithms in [14], [15], [23] are only applicable to ground robots moving in the plane and there is need to further study the control design for angle-constrained formations in 3-D using direction-only measurements.

Motivated by the application of 3-D multiagent formations using direction-only measurements, we develop 3-D angle rigidity in this article. First, we show the selection of angle constraints to

Manuscript received 27 January 2022; revised 26 July 2022 and 14 December 2022; accepted 30 December 2022. Date of publication 17 January 2023; date of current version 27 September 2023. Recommended by Associate Editor K. Cai. *(Corresponding author: Liangming Chen.)*

Liangming Chen is with the Faculty of Science and Engineering, University of Groningen, 9747 Groningen, The Netherlands, and also with the Center for Control Science and Technology, Southern University of Science and Technology, Shenzhen 518055, China (e-mail: chenlm6@sustech.edu.cn).

Ming Cao is with the Faculty of Science and Engineering, University of Groningen, 9747 Groningen, The Netherlands (e-mail: m.cao@rug.nl).

Color versions of one or more figures in this article are available at https://doi.org/10.1109/TAC.2023.3237799.

Digital Object Identifier 10.1109/TAC.2023.3237799

construct angle rigid frameworks. Then, we investigate minimal angle rigidity and angle rigidity of convex polyhedra with angle constraints only in their surfaces. Using the developed theories, we propose formation control laws to achieve a desired angle rigid formation in 3-D using direction-only measurements. The formation is constructed iteratively through the proposed two types of vertex-addition operations starting from a triangular formation and adding each new agent into the existing formation by three new angle constraints, in which interagent communication is required for each newly added agent under the first type of vertex-addition operation. The main contributions of this work are summarized as follows:

1) The approaches of constructing and merging 3-D angle rigid frameworks are proposed. Compared with the approaches of constructing 2-D angle rigid frameworks [13], [14], a sequential construction approach is developed for 3-D angle rigid frameworks. Compared with algebraic conditions for checking angle rigidity developed for 2-D and 3-D frameworks in [24] and general d-dimensional frameworks in [15], our proposed construction method provides a topological checking condition. Moreover, the merging operation on two angle rigid frameworks is also developed.
2) Angle rigidity of convex polyhedra is discussed. Rigidity of convex polyhedra is one of the oldest geometric problems [1], [2], [25]. The existing literature focuses on distance rigidity of convex polyhedra and the problem of angle rigidity of convex polyhedra has not been investigated so far. In this work, several topological conditions are developed to guarantee rigidity of convex polyhedra with angle constraints.
3) Control laws using direction-only measurements are proposed to stabilize 3-D angle rigid formations. Compared with [13], [24], where the measurements of interagent relative positions are needed, our proposed control laws only require direction measurements. Compared with [13], [14], [15], [23], where the agents lie in a 2-D plane, our proposed control laws are designed for agents moving in a 3-D space and their corresponding stability analysis is more challenging. Compared with [11], [12], [26], [27], where the desired bearing rigid formation (resp. designed bearing-based control law) relies on agents' coordinate frames, our desired angle rigid formation (resp. designed angle-based control law) is independent of agents' coordinate frames.

The rest of this article is organized as follows. Section II introduces the preliminaries. Section III presents the 3-D angle rigidity. In Section IV, the application to 3-D multiagent formations using direction-only measurements is investigated. Simulation examples are provided in Section V. Finally, Section VI concludes this article.

II. Preliminaries

A. Notations

Consider a 3-D multipoint framework and use the vertex set $\mathcal{V} = \{1, 2, \ldots, N\}$ to denote the set of indices of $N \geq 3$ vertices. Consider the embedding of the vertex set $\mathcal{V}$ in $\mathbb{R}^3$ through which each vertex i is associated with a *distinct* position $p_i \in \mathbb{R}^3$ and let $p = [p_1^{\mathrm{T}}, \ldots, p_N^{\mathrm{T}}]^{\mathrm{T}} \in \mathbb{R}^{3N}$ be the configuration of all the vertices. Let I_m, $\times$, $\lambda_{\max}$, and $\lambda_{\min}$ be the m-by-m identity matrix, the cross product, the maximum eigenvalue, and the minimum eigenvalue of a symmetric matrix, respectively. A triangle, surface, polyhedron, and angle-constrained framework are denoted by $\triangle$, $\mathbb{S}$, $\mathbb{P}$, and $\mathbb{A}$, respectively.

B. Angularity

Since each angle is associated with three vertices and an edge of a graph is only associated with two vertices, the description of angle-constrained frameworks by using graphs associated with edges of two vertices is less convenient, which motivates us to use "angularities" as has been done in [14]. Now, we extend the notion of 2-D angularity defined in [14] to 3-D. First, an *angle set* $\mathcal{A} \subset \mathcal{V} \times \mathcal{V} \times \mathcal{V}$ is the set $\{(j, i, k), j, i, k \in \mathcal{V}, j \neq i \neq k\}$, of which each element is a triplet. Each such triplet (j, i, k) will be used in this article to denote an angle formed by the vertices j, i, and k, and by confining the magnitude of the angles, one can effectively enforce an angle constraint. We denote the number of elements of the angle set $\mathcal{A}$ by $|\mathcal{A}|$. Then, the combination of the vertex set $\mathcal{V}$, the angle set $\mathcal{A}$, and the position vector p is called an *angularity*, which we denote by $\mathbb{A}(\mathcal{V}, \mathcal{A}, p)$. An element (j, i, k) in $\mathcal{A}$, when p_i, p_j, and p_k are distinct, corresponds to the interior angle formed by the rays $\overrightarrow{ij}$ and $\overrightarrow{ik}$; more specifically, using the position vector p, the angle $\measuredangle jik \in [0, \pi]$ corresponding to the triplet (j, i, k) in $\mathcal{A}$ can be calculated by

$$\measuredangle jik = \arccos\left(b_{ij}^{\top} b_{ik}\right) \tag{1}$$

where $\measuredangle jik = \measuredangle kij$, the unit vector $b_{ij} := (p_j - p_i)/l_{ij}$ represents the direction $\overrightarrow{ij}$, and $l_{ij} := \|p_j - p_i\|$.

Remark 1: The 2-D angle in [14] is calculated using the counterclockwise direction. However, the definition of each 3-D angle's direction depends on the associated vertices' coordinate frames, which are not assumed to be aligned and known in this 3-D angle rigidity. Although the 3-D angle defined in (1) does not need the notion of being counterclockwise, the 3-D angle constraints will rely on similar notions to be defined later.

III. 3-D Angle Rigidity

In this section, we first introduce 3-D angle rigidity, then introduce the merging operation for two angle rigid angularities, and in the end discuss angle rigidity of convex polyhedra. All the discussions are confined to 3-D and the right-hand rule applies to all rotation operations of vectors.

A. Angle Rigidity

Before defining angle rigidity, we first define the relations of equivalence and congruence for two angularities.

Definition 1 [14]: We say two angularities $\mathbb{A}(\mathcal{V}, \mathcal{A}, p)$ and $\mathbb{A}'(\mathcal{V}, \mathcal{A}, p')$ in 3-D with the same $\mathcal{V}$ and $\mathcal{A}$ are *equivalent* if

$$\measuredangle jik(p_j, p_i, p_k) = \measuredangle jik\left(p'_j, p'_i, p'_k\right) \quad \text{for all } (j, i, k) \in \mathcal{A}.$$

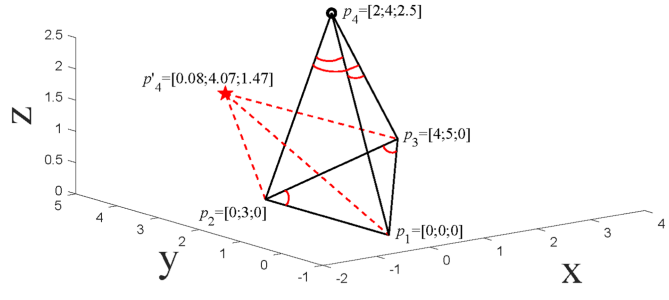

Fig. 1. Flex ambiguity in an angle rigid angularity.

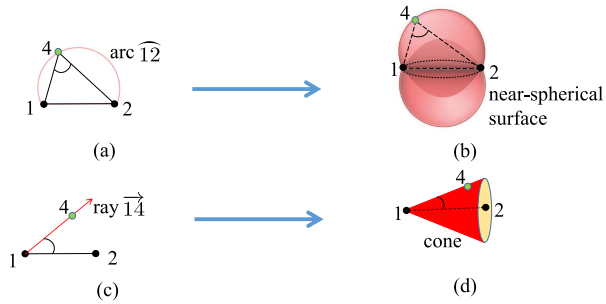

Fig. 2. Extension of angle constraints from 2-D to 3-D. (a) 2D angle $\measuredangle 142$. (B) 3D angle $\measuredangle 142$. (C) 2D angle $\measuredangle 214$. (D) 3D angle $\measuredangle 214$.

Definition 2 [14]: We say that $\mathbb{A}$ and $\mathbb{A}'$ are *congruent* if

$$\measuredangle jik(p_j, p_i, p_k) = \measuredangle jik\left(p'_j, p'_i, p'_k\right) \quad \text{for all } j, i, k \in \mathcal{V}.$$

According to Definitions 1 and 2, two equivalent (resp. congruent) angularities' corresponding angles defined in $\mathcal{A}$ (resp. all the angles defined in $\mathcal{V} \times \mathcal{V} \times \mathcal{V}$) have the same value. Now, we can define global angle rigidity and angle rigidity.

Definition 3 [14]: An angularity $\mathbb{A}(\mathcal{V}, \mathcal{A}, p)$ in 3-D is *globally angle rigid* if every angularity that is equivalent to it is also congruent to it.

Definition 4 [14]: An angularity $\mathbb{A}(\mathcal{V}, \mathcal{A}, p)$ in 3-D is *angle rigid* if there exists an $\epsilon > 0$ such that every angularity $\mathbb{A}'(\mathcal{V}, \mathcal{A}, p')$ that is equivalent to it and satisfies $\|p' - p\| < \epsilon$, is also congruent to it.

According to Definitions 3 and 4, global angle rigidity always implies angle rigidity, but the inverse is not necessarily true. This is different from bearing rigidity for which global bearing rigidity and bearing rigidity are equivalent [10], [11], [28].

Theorem 1: An angle rigid angularity $\mathbb{A}(\mathcal{V}, \mathcal{A}, p)$ in 3-D is not necessarily globally angle rigid.

Proof: We prove this theorem by constructing an angularity that is angle rigid but not globally angle rigid. Consider the angularity $\mathbb{A}(\mathcal{V}, \mathcal{A}, p)$ in Fig. 1 with $\mathcal{V} = \{1, 2, 3, 4\}$, $\mathcal{A} = \{(1, 3, 2), (3, 2, 1), (1, 4, 2), (1, 4, 3), (2, 4, 3)\}$, and the embedding $p_1 = [0, 0, 0]^{\mathrm{T}}, p_2 = [0, 3, 0]^{\mathrm{T}}, p_3 = [4, 5, 0]^{\mathrm{T}}, p_4 = [2, 4, 2.5]^{\mathrm{T}}$. The corresponding angles $\measuredangle 132, \measuredangle 321, \measuredangle 142, \measuredangle 341, \measuredangle 243$ can be calculated via (1).

We first check whether $\mathbb{A}(\mathcal{V}, \mathcal{A}, p)$ is angle rigid. In $\triangle 123$, one can uniquely determine $\measuredangle 213 = \pi - \measuredangle 132 - \measuredangle 321$, which implies that the interior angles in $\triangle 123$ are uniquely determined. If point 4's position could be uniquely determined by $\measuredangle 142, \measuredangle 143, \measuredangle 243$, the other angles formed by 4 and 1,2,3 would also be uniquely determined. To check the uniqueness of point 4 under $\measuredangle 142, \measuredangle 143, \measuredangle 243$, we first show the surface which satisfies the angle constraint of $\measuredangle 142$ given points 1 and 2. Since a 2-D angle constraint $\measuredangle 142$ allows point 4 to be in an arc $\widehat{12}$ [see Fig. 2(a)], the angle constraint of $\measuredangle 142$ in 3-D gives rise to a closed surface [see Fig. 2(b)] formed by rotating the arc $\widehat{12}$ along the line $\overline{12}$ in Fig. 2(a). Given points 1, 2, and 3 and angles $\measuredangle 142, \measuredangle 143, \measuredangle 243$, point 4 can be determined by three such surfaces. By numerically checking the intersections of these three surfaces in Fig. 3(a), one can see that there are four separate points of intersection [see Fig. 3(b)] in these three

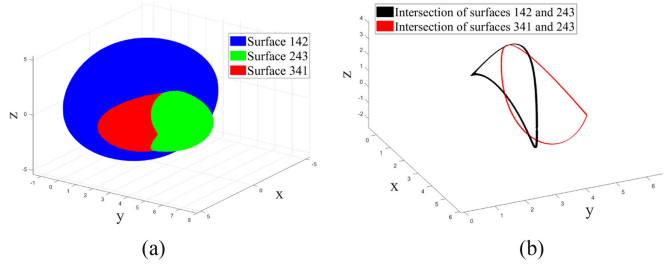

Fig. 3. Intersection of three surfaces. (a) Three surfaces. (b) Surfaces' intersected curves.

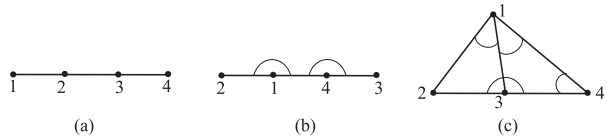

Fig. 4. Nongeneric p changes rigidity.

surfaces. Therefore, when p_1, p_2, p_3, p_4 are locally perturbed, there is only one unique position for point 4 in the neighborhood of its current position because these four intersection points are separate. More specifically, there always exists a sufficiently small perturbation (corresponding to ϵ in Definition 4) such that every perturbed angularity satisfying the given five angle constraints is congruent to $\mathbb{A}$, i,e., $\mathbb{A}$ is angle rigid.

We now show that $\mathbb{A}(\mathcal{V}, \mathcal{A}, p)$ is not globally angle rigid. Perturbing p_4 in $\mathbb{R}^3$, one finds another point $p'_4 = [0.0802, 4.0778, 1.4765]^{\mathrm{T}}$ satisfying all the angle constraints associated with $\mathcal{A}$ together with p_1, p_2, p_3, but $\measuredangle 412 = 0.675 \neq \measuredangle 4'12 = 0.348$. This flex ambiguity shown in Fig. 1 implies that $\mathbb{A}$ is not globally angle rigid.

Note that nongeneric embeddings of p in $\mathbb{R}^3$ may change rigidity properties. Now, we consider three different embeddings of a four-vertex angularity. When $\measuredangle 213 = 0, \measuredangle 143 = 0$ as shown in Fig. 4(a), the angularity is angle rigid but not globally angle rigid since if 2 and 3 swap their positions, $\measuredangle 213, \measuredangle 143$ remain the same but $\measuredangle 234$ changes by π. On the other hand, Fig. 4(b) shows that when the same two angles are assigned to be $\measuredangle 213 = \pi, \measuredangle 143 = \pi$, the angularity becomes globally angle rigid according to Definition 3. Note that in the above two cases, all the four points are collinear. When only three points are collinear as in Fig. 4(c), this angularity

is in general flexible if fewer than four angle constraints are given according to 2-D angle rigidity [14, Th. 3] since points 1,2,3,4 are in a plane in this case. By giving three generic angles (e.g., not 0 or π) for $\measuredangle 213, \measuredangle 143, \measuredangle 413$ and one nongeneric angle $\measuredangle 234 = \pi$ in Fig. 4(c), the angularity becomes globally angle rigid because $\measuredangle 124 = \pi - \measuredangle 213 - \measuredangle 143 - \measuredangle 413$, $\measuredangle 132 = \measuredangle 413 + \measuredangle 143$, and $\measuredangle 134 = \pi - \measuredangle 132$ are all uniquely determined. However, four vertices in general form a tetrahedron in 3-D. To rule out nongeneric situations for p, the notion of generic positions can be used. Following [7, Sec. 1.2], we say p is a generic position vector if its components are algebraically independent. We say an angularity $\mathbb{A}(\mathcal{V}, \mathcal{A}, p)$ is *generically (globally) angle rigid* if p is generic and $\mathbb{A}$ is (globally) angle rigid; please refer to [7], [29] for more properties of generic rigidity.

Since an angle rigid angularity is not necessarily globally angle rigid, 3-D angle rigidity is a local property, which is not related to the number of angle constraints imposed on a specific angularity. However, if one wants to construct an angle rigid structure efficiently, the number of angle constraints and their distributions within an angularity become central, which motivates us to develop sufficient conditions to guarantee global angle rigidity. First, for two angularities $\mathbb{A}(\mathcal{V}, \mathcal{A}, p)$ and $\mathbb{A}'(\mathcal{V}', \mathcal{A}', p')$, we say $\mathbb{A}$ is a *subangularity* of $\mathbb{A}'$ if $\mathcal{V} \subset \mathcal{V}'$, $\mathcal{A} \subset \mathcal{A}'$ and p is the corresponding subvector of p'. For the smallest angularities with only three vertices, there is no difference between generic angle rigidity and generic global angle rigidity.

Lemma 1 [14]: If a three-vertex angularity in 3-D is generically angle rigid, it is also generically globally angle rigid.

Proof: This is straightforward by following the proof in 2-D angle rigidity [14, Lemma 1].

Now, we develop the vertex addition operations for 3-D angle rigidity to construct an angle rigid angularity from the smallest three-vertex angularity. Toward this end, we first define some related notions.

Definition 5: For a given angularity $\mathbb{A}(\mathcal{V}, \mathcal{A}, p)$, we say that

1) a new vertex i positioned at p_i is *linearly constrained* with respect to $\mathbb{A}$ if there is $j \in \mathcal{V}$ such that $p_i \neq p_j$ and p_i is constrained to be on a ray $\overrightarrow{ji}$ starting from p_j, e.g., p_4 is constrained in ray $\overrightarrow{14}$ in Fig. 2(a).
2) i is *conically constrained* with respect to $\mathbb{A}$ if there are $j, k \in \mathcal{V}$ such that $\{p_i, p_j, p_k\}$ is generic and p_i is constrained to be on a cone $\mathcal{C}_{j\to k}$ with p_j as the cone's apex and $\overrightarrow{jk}$ as the cone's axis, e.g., p_4 is constrained in cone $\mathcal{C}_{1\to 2}$ in Fig. 2(d).
3) i is *near-spherically constrained* with respect to $\mathbb{A}$ if there are $j, k \in \mathcal{V}$ such that $\{p_i, p_j, p_k\}$ is generic and p_i is constrained to be on a near-spherical surface $\mathcal{S}_{jk}$ with $\overline{jk}$ in the surface's rotation axis, e.g., p_4 is constrained in near-spherical surface $\mathcal{S}_{12}$ in Fig. 2(b).

For convenience, we also simply say i's angle constraint is linear, conic, and near-spherical in the above three cases, respectively.

In contrast to the linear and quadratic constraints from 2-D angles [see Fig. 2(a) and (c)], each angle constraint in 3-D generally determines a surface [see Fig. 2(b) and (d)] making computations and the exploration of its properties in 3-D more challenging.

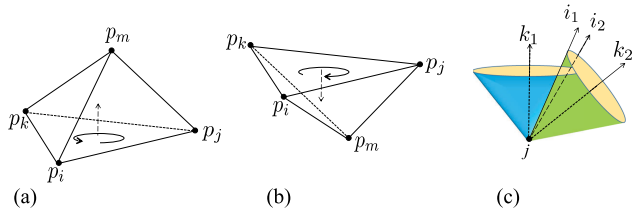

Fig. 5. Counterclockwise, clockwise, and linear constraints. (a) Counterclockwise constraint. (b) Clockwise constraint. (c) Linear constraint.

To deal with this challenge, inspired by those formation control approaches where counterclockwise direction information among agents is employed to exclude formations' ambiguities [30], [31], we also utilize counterclockwise direction constraints for 3-D angle rigidity to exclude angularities' ambiguities.

Definition 6: For four points i, j, k, m in generic positions p_i, p_j, p_k, p_m, we say m is in a counterclockwise (resp. clockwise) direction with respect to i, j, k if the signed volume of the tetrahedron formed by p_m and p_i, p_j, p_k is positive (resp. negative), i.e., $V_{m-ijk} = \frac{(p_i - p_m)^{\mathrm{T}}[(p_j - p_m)\times(p_k - p_m)]}{6} > 0$. Correspondingly, when the sign of the tetrahedron's volume is fixed to be positive (resp. negative), we say p_m is under a counterclockwise (resp. clockwise) direction constraint with respect to p_i, p_j, p_k, e.g., see Fig. 5(a) and (b).

Remark 2: As shown in Fig. 5(c), two noncoincident conic constraints $\mathcal{C}_{j\to k_1}, \mathcal{C}_{j\to k_2}$ sharing the same apex p_j will lead to two cones intersecting at no more than two rays, denoted by $\overrightarrow{ji_1}$ and $\overrightarrow{ji_2}$. Since $\overrightarrow{ji_1}$ and $\overrightarrow{ji_2}$ are symmetric with respect to the plane formed by the two cones' rotation axes $\overrightarrow{jk_1}$ and $\overrightarrow{jk_2}$, one has that $V_{i_1-jk_1k_2}$ and $V_{i_2-jk_1k_2}$ have different signs. Therefore, each linear constraint can be obtained by two conic constraints with a common apex and an associated counterclockwise constraint.

Motivated by Henneberg's construction which has been seen as a cornerstone for distance rigidity theory, we now develop two types of vertex addition operations to construct global angle rigid and angle rigid angularities in 3-D, respectively.

Definition 7 (Type-I vertex addition): For a given angularity $\mathbb{A}(\mathcal{V}, \mathcal{A}, p)$, we say the angularity $\mathbb{A}'$ with the augmented vertex set $\{\mathcal{V} \cup \{i\}\}$ is obtained from $\mathbb{A}$ through a *Type-I vertex addition* if the new vertex i's constraints with respect to $\mathbb{A}$ contain at least one of the following two cases:

Case 1: two linear constraints $\overrightarrow{j_1i}, \overrightarrow{j_2i}$, in which $\{j_1, j_2\} \subseteq \mathcal{V}$, and $\overrightarrow{j_1i}$ and $\overrightarrow{j_2i}$ are not aligned but intersecting, see Fig. 6(a);

Case 2: one linear constraint $\overrightarrow{j_1i}$ and one conic constraint $\mathcal{C}_{j_1\to j_2}$, in which $\{j_1, j_2\} \subseteq \mathcal{V}$, and $\overrightarrow{j_1i}$ and $\overrightarrow{j_1j_2}$ are not aligned but intersecting, see Fig. 6(b).

Definition 8 (Type-II vertex addition): For a given angularity $\mathbb{A}(\mathcal{V}, \mathcal{A}, p)$, we say the angularity $\mathbb{A}'$ with the augmented vertex set $\{\mathcal{V} \cup \{i\}\}$ is obtained from $\mathbb{A}$ through a *Type-II vertex addition* if the new vertex i's constraints with respect to $\mathbb{A}$ contain at least one of the following two cases:

Case 1: three near-spherical constraints $\mathcal{S}_{j_1j_2}, \mathcal{S}_{j_1k_1}, \mathcal{S}_{j_2k_1}$ with generic $\{p_i, p_{j_1}, p_{j_2}, p_{k_1}\}$ and $\{j_1, j_2, k_1\} \subseteq \mathcal{V}$, see Fig. 6(c).

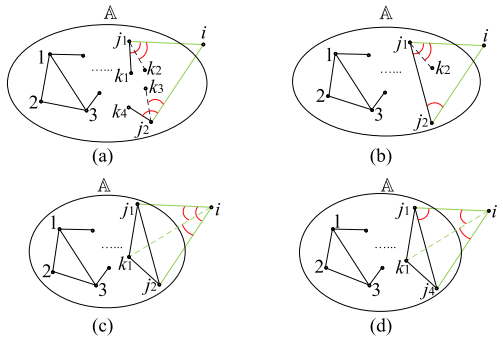

Fig. 6. Type-I vertex addition and Type-II vertex addition. (a) Case 1 in Type-I vertex addition. (b) Case 2 in Type-I vertex addition. (c) Case 1 in Type-II vertex addition. (d) Case 2 in Type-II vertex addition.

Case 2: two near-spherical constraints $\mathcal{S}_{j_1k_1}, \mathcal{S}_{j_4k_1}$ and one conic constraint $\mathcal{C}_{j_1 \to j_4}$ with generic $\{p_i, p_{j_1}, p_{j_4}, p_{k_1}\}$ and $\{j_1, j_4, k_1\} \subseteq \mathcal{V}$, see Fig. 6(d).

Now, we are ready to present a sufficient condition for global angle rigidity using Type-I vertex addition.

Proposition 1: An angularity in 3-D is globally angle rigid if it can be obtained through a sequence of Type-I vertex additions starting from a generically angle rigid three-vertex angularity.

Proof: According to Lemma 1, a generically angle rigid three-vertex angularity is globally angle rigid. Consider the two cases in the Type-I vertex addition given in Definition 7. If case 1 applies, each linear constraint corresponds to a ray according to Definition 6. Then, the position p_i of the newly added vertex i is unique since two rays, not aligned, starting from two different points may intersect only at one point; if case 2 applies, p_i is again unique since a ray starting from the axis of a cone can have only one intersection with the cone. Therefore, p_i is always globally uniquely determined, after which all the involved angles are also globally uniquely determined. Then, iteratively, after a sequence of type-I vertex additions, the obtained angularity is globally angle rigid.

In comparison, type-II vertex additions can only guarantee angle rigidity instead of global angle rigidity.

Proposition 2: An angularity in 3-D is angle rigid if it can be obtained through a sequence of Type-II vertex additions starting from a generically angle rigid three-vertex angularity.

The proof can be easily constructed following similar arguments as those for Proposition 1 and Theorem 1. The only difference is that p_i now may have multiple isolated solutions and is only unique locally. Also, note that only two types of constraints are defined in Type-II vertex addition operation in Definition 8, but there are more possible combinations of constraints which can also guarantee a locally unique point p_i.

Corollary 1: For an angularity $\mathbb{A}(\mathcal{V}, \mathcal{A}, p)$, if there exists an angle rigid (resp. globally angle rigid) subangularity $\mathbb{A}'(\mathcal{V}, \mathcal{A}', p)$ with $\mathcal{A}' \subset \mathcal{A}$, then $\mathbb{A}(\mathcal{V}, \mathcal{A}, p)$ is also angle rigid (resp. globally angle rigid).

Proof: Since the vertex set in the subangularity $\mathbb{A}'$ is the same as $\mathbb{A}$, one has from Definitions 3 and 4 that angle rigidity of the subangularity $\mathbb{A}'$ implies angle rigidity of $\mathbb{A}$.

Remark 3: The associated counterclockwise direction constraint introduced in Definition 6 can be used to remove the reflection ambiguity such that the position of the added vertex i in the Type-I vertex addition operation (see Definition 7) can be globally uniquely determined. But this constraint is not sufficient to make the position of the added point in Type-II vertex addition operation (see Definition 8) globally uniquely determined. An example is given in Fig. 1, where points 1, 2, 3 are in the clockwise direction with respect to both points 4 and 4'. In other words, not only reflection ambiguity but also flex ambiguity may exist in Type-II vertex addition operation.

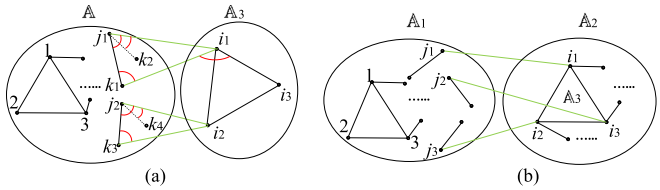

Fig. 7. Three-vertex addition operation and merging operation.

Remark 4: Note that Propositions 1 and 2 can also be used as topological conditions to check global angle rigidity and angle rigidity of angularities that can be sequentially constructed from a triangle, respectively. For those angularities that are not constructed through such sequential operations, rank-based algebraic conditions can be employed to check their infinitesimal or generic angle rigidity when the corresponding angularities' embedding p is known [15, Th. 3].

B. Merging two Angle Rigid Angularities

After introducing how to add one vertex to an angularity in Propositions 1 and 2, we now investigate how to add three vertices to an angularity [see Fig. 7(a)], which becomes useful later for merging two angle rigid angularities.

Definition 9 (Three-vertex addition operation): For a given angularity $\mathbb{A}(\mathcal{V}, \mathcal{A}, p)$ and three new vertices $\{i_1, i_2, i_3\} \nsubseteq \mathcal{V}$, we say that the angularity $\mathbb{A}'$ with the augmented vertex set $\{\mathcal{V} \cup \{i_1, i_2, i_3\}\}$ is obtained from $\mathbb{A}$ through a *three-vertex addition operation* if the new vertices' constraints with respect to $\mathbb{A}$ contain: two unaligned linear constraints $\overrightarrow{j_1 i_1}, \overrightarrow{k_1 i_1}$, two unaligned linear constraints $\overrightarrow{j_2 i_2}, \overrightarrow{k_3 i_2}$, and one conic constraint $\mathcal{C}_{i_1 \to k_1}$ and one associated counterclockwise constraint $V_{i_3 - i_2 i_1 k_1}$ for i_3, in which $\{j_1, j_2, k_1, k_3\} \subseteq \mathcal{V}$. We further denote the angle set corresponding to these added angle constraints by $\mathcal{A}^{\{i_1, i_2, i_3\}}$.

Now, we merge a three-vertex generically angle rigid angularity to a globally angle rigid angularity by the three-vertex addition operation [see Fig. 7(a)].

Proposition 3: For a globally angle rigid angularity $\mathbb{A}(\mathcal{V}, \mathcal{A}, p)$ and a three-vertex generically angle rigid angularity $\mathbb{A}_3\left(\{i_1, i_2, i_3\}, \mathcal{A}_3, [p_{i_1}^{\mathrm{T}}, p_{i_2}^{\mathrm{T}}, p_{i_3}^{\mathrm{T}}]^{\mathrm{T}}\right)$, if one merges $\mathbb{A}$ and $\mathbb{A}_3$ by adding the vertices i_1, i_2, i_3 to $\mathbb{A}$ through the three-vertex addition operation, then the merged angularity $\mathbb{A}'\left(\mathcal{V} \cup \{i_1, i_2, i_3\}, \mathcal{A} \cup \mathcal{A}_3 \cup \mathcal{A}^{\{i_1, i_2, i_3\}}, \left[p^{\mathrm{T}}, p_{i_1}^{\mathrm{T}}, p_{i_2}^{\mathrm{T}}, p_{i_3}^{\mathrm{T}}\right]^{\mathrm{T}}\right)$ is globally angle rigid.

Proof: Note that the positions of the added vertices i_1 and i_2 are globally unique according to Proposition 1 (case 1 of Type I vertex addition). After p_{i_1} and p_{i_2} are fixed, the vertex

i_3 is constrained on the intersection of two cones with $\overline{i_1 i_2}$ as these two cones' rotation axis because $\mathbb{A}_3$ is generically angle rigid and $\measuredangle i_3 i_1 i_2$ and $\measuredangle i_3 i_2 i_1$ are fixed. By further using the given conic constraint for i_3 together with the associated counterclockwise constraint, one has that the position of the added vertex i_3 is also globally unique according to Proposition 1 (case 2 of Type-I vertex addition).

Since the vertex set and the embedding of $\mathbb{A}$ are different from those of $\mathbb{A}'$, Corollary 1 cannot be used as the the proof of Proposition 3. Fig. 7(a) shows the original angle constraints to realize the three-vertex addition operation. According to [15] and [24], the minimum number of angle constraints to guarantee an N-node angle-constrained framework's angle rigidity is $3N-7$. Therefore, the number of these angle constraints in Fig. 7(a) is 7 because the total degrees of freedoms for vertices i_1, i_2, i_3 in 3-D is 9, and at least two angle constraints are needed to make $\mathbb{A}_3$ generically angle rigid. Thus, at least 9-2=7 angle constraints related to i_1, i_2, i_3 are needed to merge $\mathbb{A}_3$ with $\mathbb{A}$. Definition 9 only gives one set of angle constraints for merging operation under global angle rigidity, and there are many other acceptable sets, especially when the number of angle constraints is larger than 7 or the merged angularity is only required to be angle rigid. Now, we discuss how to merge two angle rigid angularities as shown in Fig. 7(b).

Proposition 4: Suppose that the angularity $\mathbb{A}_1(\mathcal{V}_1, \mathcal{A}_1, p)$ is globally angle rigid and $\mathbb{A}_2(\mathcal{V}_2, \mathcal{A}_2, p')$ with $\mathcal{V}_1 \cap \mathcal{V}_2 = \varnothing$ has a subangularity $\mathbb{A}_2'(\mathcal{V}_2, \mathcal{A}_2', p')$ which can be obtained through a sequence of Type-I vertex additions from a generically angle rigid three-vertex angularity $\mathbb{A}_3\left(\{i_1, i_2, i_3\}, \mathcal{A}_3, \left[p_{i_1}^{\mathrm{T}}, p_{i_2}^{\mathrm{T}}, p_{i_3}^{\mathrm{T}}\right]^{\mathrm{T}}\right)$. If one merges $\mathbb{A}_1$ and $\mathbb{A}_2$ by adding the vertices i_1, i_2, i_3 to $\mathbb{A}_1$ through the three-vertex addition operation, then the merged angularity $\mathbb{A}''\left(\mathcal{V}_1 \cup \mathcal{V}_2, \mathcal{A}_1 \cup \mathcal{A}_2 \cup \mathcal{A}^{\{i_1,i_2,i_3\}}, \left[p^{\mathrm{T}}, p'^{\mathrm{T}}\right]^{\mathrm{T}}\right)$ is globally angle rigid.

Proof: According to Proposition 3, adding the vertices i_1, i_2, i_3 to $\mathbb{A}_1$ through the three-vertex addition operation yields global angle rigidity of the merged angularity with augmented vertex set $\{\mathcal{V}_1 \cup \{i_1, i_2, i_3\}\}$. According to Proposition 1, Since $\mathbb{A}_2'$ can be obtained through a sequence of Type-I vertex additions from $\mathbb{A}_3$, one has global angle rigidity of the angularity $\mathbb{A}_{1-2}'\left(\mathcal{V}_1 \cup \mathcal{V}_2, \mathcal{A}_1 \cup \mathcal{A}_2' \cup \mathcal{A}^{\{i_1,i_2,i_3\}}, \left[p^{\mathrm{T}}, p'^{\mathrm{T}}\right]^{\mathrm{T}}\right)$ after merging $\mathbb{A}_1$ and $\mathbb{A}_2'$. Because the angularity $\mathbb{A}_{1-2}'$ is a subangularity of $\mathbb{A}''$, the merged angularity $\mathbb{A}''$ is globally angle rigid according to Corollary 1.

C. Minimal Angle Rigidity

Minimal angle rigidity plays an important role in deriving angle rigidity's necessary and sufficient conditions. Inspired by Laman theorem for 2-D distance-constrained frameworks, we now present some results on 3-D infinitesimal minimal angle rigidity, whose definition is the same as [14, Definitions 9 and 10] after replacing 2-D by 3-D. Thus, for more details about the definition of infinitesimal minimal angle rigidity, we refer the readers to [14].

Lemma 2: A 3-D angularity $\mathbb{A}(\mathcal{V}, \mathcal{A}, p)$ is infinitesimally minimally angle rigid if and only if it is infinitesimally angle rigid and $|\mathcal{A}| = 3|\mathcal{V}| - 7$.

The proof of Lemma 2 follows straightforwardly from the fact that the magnitude of each 3-D angle is invariant under its associated vertices' overall translation, rotation, and scaling.

Lemma 3: A 3-D infinitesimally minimally angle rigid angularity must have a vertex associated with more than 2 but fewer than 9 angle constraints.

From Lemma 2, the proof of Lemma 3 can be obtained straightforwardly by following the proof of [14, Lemma 4]. However, according to Lemma 3, there are six cases for the number of the vertex's associated constraints, which makes it challenging to use Laman's induction method to get a necessary condition for angle rigidity. Instead, we focus on a special class of angularity, namely tetrahedral angularity whose angle set $\mathcal{A}$ is a tetrahedral angle set. We say $\mathcal{A}$ is a *triangular angle set* if for every $(i_1, j_1, k_1) \in \mathcal{A}$, there also exists $\{(j_1, k_1, i_1), (k_1, i_1, j_1)\} \subset \mathcal{A}$. We say $\mathcal{A}$ is a *tetrahedral angle set* if $\mathcal{A}$ is a triangular angle set and for every triangular angle subset $\mathcal{T}_{\triangle i_1 j_1 k_1} := \{(i_1, j_1, k_1), (j_1, k_1, i_1), (k_1, i_1, j_1)\} \in \mathcal{A}$, there always exists a vertex $m \in \mathcal{V}$, $m \neq i_1 \neq j_1 \neq k_1$ such that $\mathcal{T}_{\triangle i_1 j_1 m} \in \mathcal{A}$, $\mathcal{T}_{\triangle i_1 k_1 m} \in \mathcal{A}$, $\mathcal{T}_{\triangle j_1 k_1 m} \in \mathcal{A}$. We say $\{\mathcal{T}_{\triangle i_1 j_1 k_1}, \mathcal{T}_{\triangle i_1 j_1 m}, \mathcal{T}_{\triangle i_1 k_1 m}, \mathcal{T}_{\triangle j_1 k_1 m}\}$ is a tetrahedral angle subset corresponding to tetrahedron $\triangle m i_1 j_1 k_1$.

Definition 10: An angularity $\mathbb{A}(\mathcal{V}, \mathcal{A}, p)$ is said to be infinitesimally minimally and tetrahedrally angle rigid if $\mathcal{A}$ is a tetrahedral angle set, $\mathbb{A}$ is infinitesimally angle rigid and fails to remain so after removing any tetrahedron in $\mathcal{A}$.

Let $n_{\mathcal{A}}^{\triangle} \in \mathbb{N}$ be the number of tetrahedra in the tetrahedral angle set $\mathcal{A}$. Let $\bar{\mathcal{A}}$ be the multiset satisfying that each element of $\bar{\mathcal{A}}$ is a triplet, $\bar{\mathcal{A}}$ consists of $n_{\mathcal{A}}^{\triangle}$ tetrahedral angle subset of $\mathcal{A}$, $|\bar{\mathcal{A}}| = 3 * 4 * n_{\mathcal{A}}^{\triangle}$, and duplicate elements may exist in $\bar{\mathcal{A}}$.

Proposition 5: For an infinitesimally minimally and tetrahedrally angle rigid angularity $\mathbb{A}(\mathcal{V}, \mathcal{A}, p)$, one has that $n_{\mathcal{A}}^{\triangle} = \lceil \frac{3|\mathcal{V}|-7}{5} \rceil$, and $\mathbb{A}$ must have a vertex associated with one or two tetrahedra in $\bar{\mathcal{A}}$.

Proof: First, we prove $n_{\mathcal{A}}^{\triangle} = \lceil \frac{3|\mathcal{V}|-7}{5} \rceil$. From Lemma 2, angle rigid angularities' minimum number of independent angle constraints (the definition of independent angles is given in [14, Definition 8]) is $3|\mathcal{V}| - 7$. Since each tetrahedron has five independent angle constraints, one has $n_{\mathcal{A}}^{\triangle} = \lceil \frac{3|\mathcal{V}|-7}{5} \rceil$. Then, we prove $\mathbb{A}$ must have a vertex associated with one or two tetrahedra. Suppose on the contrary that each vertex is associated with at least three tetrahedra in $\bar{\mathcal{A}}$. Since $\bar{\mathcal{A}}$ is a tetrahedral angle set and each vertex m will show up nine times in its associated tetrahedral angle subset $\{\mathcal{T}_{\triangle i_1 j_1 k_1}, \mathcal{T}_{\triangle i_1 j_1 m}, \mathcal{T}_{\triangle i_1 k_1 m}, \mathcal{T}_{\triangle j_1 k_1 m}\}$, all the vertices' appearance times in $\bar{\mathcal{A}}$ will be at least $3 * 9 * |\mathcal{V}|$. However, the set $\bar{\mathcal{A}}$ only has $3 * 4 * n_{\mathcal{A}}^{\triangle}$ triples, i.e., all the vertices' total appearance times in $\bar{\mathcal{A}}$ are $3 * 12 * n_{\mathcal{A}}^{\triangle}$. Since $36 n_{\mathcal{A}}^{\triangle} = 36 \lceil \frac{3|\mathcal{V}|-7}{5} \rceil < 27|\mathcal{V}|$, this implies a contradiction, for which $\mathbb{A}$ must have a vertex associated with one or two tetrahedra.

Although there are only two cases for the number of the vertex's associated tetrahedra in an infinitesimally, minimally and tetrahedrally angle rigid angularity, the combinatory form of those tetrahedra with respect to the other vertices in $\mathcal{V}$ is multiple, which makes it challenging to obtain a similar conclusion like Laman's theorem. Nevertheless, the conclusions presented in this section can be a foundation for further investigation of 3-D minimal angle rigidity.

D. Angle Rigidity of Convex Polyhedra

As is well known, distance rigidity of convex polyhedra is one of the oldest geometric problems and has been studied by Euler [1], Cauchy [2], and Gluck [25], to name a few. Although many distance rigidity-related results have been obtained for convex polyhedra, the problem of angle rigidity of convex polyhedra[1] has not been investigated so far. Instead of using edge-based frameworks, we use angularities introduced in Section II-B to describe polyhedra with angle constraints.

For a convex polyhedron $\mathbb{P}$, we define the corresponding angularity $\mathbb{A}(\mathcal{V},\mathcal{A},p)$, where $\mathcal{V}$ is the vertex set consisting of all the vertices of $\mathbb{P}$, $\mathcal{A}$ is the angle set consisting of all the angles[2] of the faces of $\mathbb{P}$, and p is the position vector of the 3-D embedding of the vertices in $\mathcal{V}$. Define the *angle function* $f_{\mathcal{A}}(p):=[f_1,\ldots,f_{|\mathcal{A}|}]^{\mathrm{T}}\in\mathbb{R}^{|\mathcal{A}|}$ for the angularity $\mathbb{A}(\mathcal{V},\mathcal{A},p)$ where $f_m:\mathbb{R}^9\to[0,\pi]$, $m=1,\ldots,|\mathcal{A}|$, is the mapping from $[p_i^{\mathrm{T}},p_j^{\mathrm{T}},p_k^{\mathrm{T}}]^{\mathrm{T}}$ of the mth element (i,j,k) in $\mathcal{A}$ to the angle $\measuredangle ijk$. The main difference between this section and the previous sections is that the angle constraints of a polyhedron are not in a cascading sequence, but all on its surfaces.

Lemma 4 ([32], Sec. 10.3.2, Th. 1): If all angles on the faces of a convex polyhedron $\mathbb{P}$ remain constant when $\mathbb{A}$ is perturbed, then all the dihedral angles of $\mathbb{P}$ remain constant.

Lemma 5 ([32], Sec. 10.4.1, Th. 1): If all edge lengths, angles in faces, and dihedral angles of a convex polyhedron $\mathbb{P}$ remain constant under a perturbation of $\mathbb{A}$, then the perturbation must be a translation or rotation of $\mathbb{A}$.

With the properties of the perturbation provided in Lemmas 4 and 5, we now provide a specific class of $\mathcal{A}$ such that these properties can be used for angle rigidity of convex polyhedra.

Theorem 2: The angularity $\mathbb{A}(\mathcal{V},\mathcal{A},p)$ obtained from a convex polyhedron $\mathbb{P}$ with all faces being triangles is angle rigid.

Proof: Following Definition 1, we consider $\mathbb{A}$'s equivalent angularity $\mathbb{A}'(\mathcal{V},\mathcal{A},p')$ with $\|p'-p\|<\epsilon,\epsilon>0$, and denote by $\mathbb{P}'$ the corresponding polyhedron. Since $\mathbb{A}$ and $\mathbb{A}'$ are equivalent, each two corresponding face angles in $\mathbb{A}$ and $\mathbb{A}'$ have the same value (i.e., $f_{\mathcal{A}}(p)=f_{\mathcal{A}}(p')$). According to Lemma 4, one has that each two corresponding dihedral angles formed by two adjacent faces in $\mathbb{P}$ and $\mathbb{P}'$ have the same value.

Considering an arbitrary face triangle $\triangle ijk,i,j,k\in\mathcal{V}$, one has $\triangle ijk(p_i,p_j,p_k)\sim\triangle ijk(p'_i,p'_j,p'_k)$. Now, we scale $\mathbb{A}'$ to obtain $\mathbb{A}''$, which satisfies $\|p_i-p_j\|=\|p''_i-p''_j\|$, $\|p_i-p_k\|=\|p''_i-p''_k\|$ and $\|p_k-p_j\|=\|p''_k-p''_j\|$. We denote the scaled polyhedron by $\mathbb{P}''$. Since the scaling will not change all (face or dihedral) angles of a polyhedron, one has $f_{\mathcal{A}^*-\mathcal{A}}(p')=f_{\mathcal{A}^*-\mathcal{A}}(p'')$ and $f_{\mathcal{A}}(p')=f_{\mathcal{A}}(p'')$, where $\mathcal{A}^*=\{(i,j,k)|\forall i,j,k\in\mathcal{A},i\neq j\neq k\}$ is the complete angle set. Now, we check $\mathbb{A}$ and $\mathbb{A}''$. First, all the face angles have the same values in $\mathbb{A}$ and $\mathbb{A}''$ because $f_{\mathcal{A}}(p)=f_{\mathcal{A}}(p')=f_{\mathcal{A}}(p'')$. Second, all the dihedral angles in $\mathbb{P}$ and $\mathbb{P}''$ have the same values because $\mathbb{P}$ and $\mathbb{P}'$ have the same dihedral angles and $\mathbb{A}''$ is a scaling of $\mathbb{A}'$. Third, because $\triangle ijk(p_i,p_j,p_k)\simeq\triangle ijk(p''_i,p''_j,p''_k)$, the lengths of the edges in $\mathbb{P}$ have the same values as the lengths of the corresponding edges in $\mathbb{P}''$, which can be obtained by using the law of sines iteratively for the face triangles in $\mathbb{P}$ and $\mathbb{P}''$. From the above three facts and using Lemma 5 for $\mathbb{A}$ and $\mathbb{A}''$, one has that $\mathbb{A}''$ is the translation or rotation of $\mathbb{A}$, under which the values of all triple-vertex angles remain unchanged. It follows that $f_{\mathcal{A}^*-\mathcal{A}}(p)=f_{\mathcal{A}^*-\mathcal{A}}(p'')=f_{\mathcal{A}^*-\mathcal{A}}(p')$. Therefore, $\mathbb{A}$ and $\mathbb{A}'$ are congruent, and $\mathbb{A}$ is angle rigid.

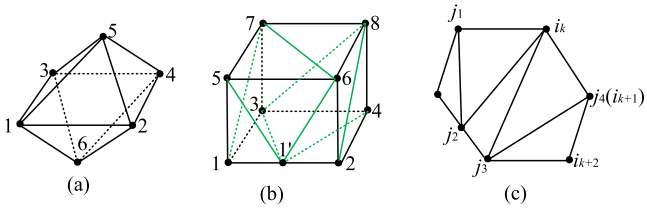

Fig. 8. Angle rigidity of convex polyhedra. (a) Convex polyhedron with triangular surfaces. (b) Surface triangulation. (c) Coplanar face.

Instead of focusing on convex polyhedra with triangular faces [see Fig. 8(a)], we now study the case of convex polyhedra whose faces are not necessarily triangles. Note that when a face is not a triangle, the face's vertices may become noncoplanar under perturbations, for which we now develop the operations of polygonal triangulation and surface triangulation.

Definition 11 (Polygonal triangulation [29]): Polygonal triangulation is the decomposition of a polygon into a set of triangles where any two of these triangles either do not intersect at all or intersect at a common vertex or edge.

Definition 12 (Surface triangulation): Surface triangulation for a polyhedron $\mathbb{P}$ is the decomposition of the surface of $\mathbb{P}$ using polygonal triangulation for each face of $\mathbb{P}$ and at the same time any two decomposed triangles from two faces of $\mathbb{P}$ either do not intersect at all or intersect at a common vertex or edge.

An example of surface triangulation is shown in Fig. 8(b). Then, we define the corresponding triangulated angularity.

Definition 13 (Triangulated polyhedral angularity): Let $\mathcal{K}$ be a surface triangulation of a polyhedron $\mathbb{P}$ with the vertex set $\mathcal{V}=\{1,2,\ldots,N\}$ and embedding $p=[p_1^{\top},\ldots,p_N^{\top}]^{\top}$. Then, we call $\mathbb{A}(\mathcal{V}\cup\mathcal{V}',\mathcal{A},[p^{\top},p'^{\top}]^{\top})$ a *triangulated polyhedral angularity*, where $\mathcal{V}'$ is the vertex set consisting of the vertices added in the surface triangulation $\mathcal{K}$, p' is the corresponding embedding of the vertices in $\mathcal{V}'$, and $\mathcal{A}$ denotes the angle set consisting of the interior angles of all polygonal faces of the polyhedron with vertices $\mathcal{V}\cup\mathcal{V}'$ and embedding $[p^{\top},p'^{\top}]^{\top}$ and

[1] We only consider closed polyhedra in this article.

[2] For a closed polyhedron, one can easily distinguish the inside that its surfaces enclose from its outside, so it is possible to define the positive directions of the faces to be the normals pointing outwards. Therefore, the angle constraints on the surfaces of such a polyhedron can be associated with the clockwise or counterclockwise directions.

all the interior angles of triangles[3] obtained by $\mathcal{K}$ for the surface of $\mathbb{P}$. Then, the polyhedron corresponding to $\mathcal{K}$ is called a triangulated polyhedron $\tilde{\mathbb{P}}$.

Note that if $\mathbb{P}$ is convex, we say its corresponding $\mathbb{A}$ is a convex triangulated polyhedral angularity. We first present two lemmas which will be needed for the proof of the main result.

Lemma 6: When locally perturbing the convex triangulated polyhedral angularity $\mathbb{A}\left(\mathcal{V}\cup\mathcal{V}',\mathcal{A},\left[p^{\top},p'^{\top}\right]^{\top}\right)$, the vertices of $\mathcal{V}\cup\mathcal{V}'$ that are on a face of $\tilde{\mathbb{P}}$ are always coplanar under the angle constraints given in $\mathcal{A}$.

Proof: We first prove that under the given angle constraints all the triangles in a face of $\tilde{\mathbb{P}}$ will be coplanar under the local perturbation. Consider an arbitrary face $\mathbb{S}$ of $\tilde{\mathbb{P}}$ whose vertices consist of $\mathcal{I}=\{i_1,\ldots,i_m\}$ where $m\geq 3$. Suppose that $i_k, 1\leq k\leq m$ is one of the vertices in $\mathbb{S}$ and is involved in face triangles $\triangle j_1 i_k j_2, \triangle j_2 i_k j_3,\ldots,\triangle j_{n-1} i_k j_n$ where $j_1,\ldots,j_n\in\mathcal{I}$ and $j_1,\ldots,j_n\neq i_k$, and an example is in Fig. 8(c). Note that if $j_1=j_{n-1}$ and $j_2=j_n$, i.e., i_k is only involved in one triangle $\triangle j_1 i_k j_2$ in $\mathbb{S}$, then one has that j_1, i_k, j_2 are coplanar since three arbitrary points in 3-D are coplanar. When i_k is involved in more than one triangle in $\mathbb{S}$, one has $\{(j_1,i_k,j_2),(j_2,i_k,j_3),\ldots,(j_{n-1},i_k,j_n)\}\in\mathcal{A}$, $(j_1,i_k,j_n)\in\mathcal{A}$ and $\measuredangle j_1 i_k j_2+\measuredangle j_2 i_k j_3+\cdots\measuredangle j_{n-1} i_k j_n=\measuredangle j_1 i_k j_n$. Since all the vertices of $\mathcal{V}$ and $\mathcal{V}$' lie on the boundary of the polyhedron, under the local perturbation, $i_k, j_1, j_2,\ldots,j_n$ must be coplanar; otherwise $\measuredangle j_1 i_k j_2+\measuredangle j_2 i_k j_3+\cdots+\measuredangle j_{n-1} i_k j_n>\measuredangle j_1 i_k j_n$, which violates the given angle constraints. Note that for each triangle $\triangle ijk$ in face $\mathbb{S}$, there always exists another triangle in face $\mathbb{S}$ that shares a common edge with $\triangle ijk$. Without loss of generality, assume that the another triangle is $\triangle ij\tilde{k}$ and the intersected edge is ij. Consider the first case that i is only involved in these two triangles in face $\mathbb{S}$. Then $\{(j,i,k),(j,i,\tilde{k})\}\in\mathcal{A}$, $(k,i,\tilde{k})\in\mathcal{A}$ and $\measuredangle jik+\measuredangle ji\tilde{k}=\measuredangle ki\tilde{k}$. Under local perturbation, these two triangles are coplanar. The second case is that i is involved in multiple triangles, using the same argument for the shared vertex as i_k, one has that these triangles are coplanar.

To prove that all the vertices in each face $\mathbb{S}$ is coplanar, we now consider that vertex i_k is involved in $n-1$ coplanar triangles in face $\mathbb{S}$, and its neighboring vertex i_{k+1} is involved in $\tilde{n}$ coplanar triangles in $\mathbb{S}$, for which an example is in Fig. 8(c). Note that those $n-1$ triangles from i_k and $\tilde{n}$ triangles from i_{k+1} must share at least one common triangle because of the existence of edge $i_k i_{k+1}$. Then, those $n+\tilde{n}-2$ triangles of i_k and i_{k+1} should be coplanar, and thus all the these triangles' vertices are coplanar. Next, if i_{k+1} has a different neighboring vertex than i_k, we consider this vertex and label it i_{k+2}. Using the previous argument again, one has that all triangles of i_k, i_{k+1}, i_{k+2} are coplanar. Using this argument repeatedly for new neighboring vertices until one reaches all vertices in $\mathcal{I}$, one has that all the triangles in $\mathbb{S}\cap\mathcal{K}$ are coplanar since the vertices of each triangle in $\mathbb{S}\cap\mathcal{K}$ lie in $\mathcal{I}$. Because all the triangles in $\mathbb{S}\cap\mathcal{K}$ cover all the vertices in $\mathcal{I}$, one has that the vertices of $\mathcal{V}\cup\mathcal{V}'$ that is in $\mathbb{S}$ are coplanar under the perturbation. The same holds for the other faces of $\tilde{\mathbb{P}}$. □

Lemma 7: When locally perturbing the convex triangulated polyhedral angularity $\mathbb{A}(\mathcal{V}\cup\mathcal{V}',\mathcal{A},[p^{\top},p'^{\top}]^{\top})$, if the scale of a triangle in a face of $\tilde{\mathbb{P}}$ remains constant, then all the edge lengths of $\tilde{\mathbb{P}}$ remain constant.

Proof: Note that after triangulating the faces of the polyhedron $\mathbb{P}$, the surface of $\tilde{\mathbb{P}}$ becomes $\mathcal{K}$, in which each triangle $\triangle ijk\in\mathcal{K}$ has three neighboring triangles and each of them shares a different edge with the triangle $\triangle ijk$. When the scale of this arbitrary triangle $\triangle ijk$ in $\mathcal{K}$ is fixed, its three neighboring triangles also have the same fixed scale using the law of sines. Now, we show why the scales of all the other triangles in $\mathcal{K}$ are fixed as well. Let the face where $\triangle ijk$ lies be $\mathbb{S}_1$ and the total number of triangles in $\mathbb{S}_1$ is m. Then, after fixing the scale of the three neighboring triangles of $\triangle ijk$, one can fix $\triangle ijk$'s neighboring triangles' neighboring triangle; such a propagating fixing process will fix the scales of all the triangles in $\mathbb{S}_1$. Now, consider $\mathbb{S}_1$'s neighboring face $\mathbb{S}_2$ that shares at least one edge with $\mathbb{S}_1$. Since the scales of all triangles in $\mathbb{S}_1$ are fixed, the length of this shared edge is fixed and the scale of the triangle containing this edge in $\mathbb{S}_2$ is also fixed. Apply for $\mathbb{S}_2$ the same argument for $\mathbb{S}_1$, all the triangles in $\mathbb{S}_2$ can be fixed. Because the polyhedron $\mathbb{P}$ is closed, under the triangulation $\mathcal{K}$, one can always fix the neighboring triangles from those triangles with fixed scale until all the triangles in $\mathcal{K}$ are fixed. Therefore, all the edge lengths are constant provided that one triangle's scale is constant. □

Now, we present the main result about the convex triangulated polyhedral angularity.

Theorem 3: A convex triangulated polyhedral angularity $\mathbb{A}(\mathcal{V}\cup\mathcal{V}',\mathcal{A},[p^{\top},p'^{\top}]^{\top})$ without any vertex of $\mathcal{V}'$ lying in the interior of a face of $\mathbb{P}$ is angle rigid.

Proof: We prove Theorem 3 following the proof of Theorem 2. According to Lemma 6, one has that the vertices of $\mathcal{V}\cup\mathcal{V}'$ that are involved in a face of $\tilde{\mathbb{P}}$ will be coplanar under the perturbation. Therefore, using Lemma 4, each corresponding dihedral angle formed by two adjacent faces keep constant under the perturbation. On the other hand, Lemma 7 implies that all the edge lengths of $\tilde{\mathbb{P}}$ keep constant under the given conditions. Based on these two facts and the proof of Theorem 2, one has that $\mathbb{A}$ is angle rigid. □

A face in a convex polyhedron is said to be infinitesimally angle rigid if the face can only translate, rotate and scale under any local perturbation. We now consider the case where each face of the convex polyhedron is infinitesimally angle rigid.

Corollary 2: A convex polyhedron with infinitesimally angle rigid faces is angle rigid.

The proof of this corollary follows the proof of Theorem 2. On the one hand, all angles in each face will remain constant under a perturbation according to the definition of infinitesimally angle rigid face. On the other hand, translation and rotation of a face will not change the lengths of its edges. When one edge length is fixed under the perturbation, the scale of the infinitesimally angle rigid face is also fixed, which implies that the lengths of the other edges of the face are fixed. Note that each face of the convex polyhedron has at least three neighboring faces and

[3]Since the sum of three interior angles of each triangle is π, each triangle has one redundant angle in the angle set.

each pair of them share a different edge with the original face. Therefore, by fixing edge length iteratively, all the edge lengths of the polyhedron will be fixed given one fixed edge length in the polyhedron. From the above two facts and Lemma 5, one has that the convex polyhedron is angle rigid.

E. Comparison With 2-D Angle Rigidity

Recently, rigidity or infinitesimal shape-similarity of 2-D angle-constrained frameworks has been investigated in [13], [14], [15]. Compared with the existing results in 2-D [13], [14], [15], the contributions of the developed 3-D angle rigidity in this article lie in three aspects. First, we show in Section III-A that each angle constraint determines a conic or near-spherical surface in 3-D, where a counterclockwise constraint is defined to avoid reflection ambiguity. Second, the approaches of constructing and merging 3-D angle rigid frameworks are proposed in Sections III-A and III-B. The proposed sequential construction approach for 3-D angle rigid and globally angle rigid frameworks can also be employed as topological conditions to check 3-D frameworks' angle rigidity. Last, angle rigidity of convex polyhedra is discussed in Section III-C, in which all the angle constraints only lie in the faces of polyhedra and no sequential construction from the given angle constraints is applicable.

IV. Application to 3-D Direction-Only Formations

In the applications of autonomous aerial refueling, drone swarm's group display, and satellite formation keeping [33], a desired 3-D formation is usually required to be formed by those teams of vehicles, where 2-D angle-based formation algorithms [13], [14], [15], [23] cannot be used. In addition, many proposed formation control algorithms require the measurements of aligned bearings [10], [34], bearings under specific coordinate frames [11], [26], or relative positions [13], [19], [24], [35]. An angle-based synthesized controller is proposed in [36], which applies to d-dimensional space and arbitrary topology if interagent distance measurements are available. In some of those applications, compared with the aligned bearing or relative position measurements, direction (or local bearing) measurements are more accessible [14], [15], [22]. Therefore, in this section, we design direction-only formation algorithms to stabilize 3-D angle rigid formations with the help of 3-D angle rigidity theory that we have just developed.

Consider a team of $N \geq 3$ agents, labeled by $1, 2, \ldots, N$, in 3-D, each of which is governed by single-integrator dynamics

$$\dot{p}_i = u_i, i = 1, \ldots, N \tag{2}$$

where $p_i \in \mathbb{R}^3$ denotes agent i's position, and $u_i \in \mathbb{R}^3$ is the control input to be designed. Each agent i can measure the directions $\overrightarrow{ij}, j \in \mathcal{N}_i$ and only communicates with its neighbors when the formation is constructed by Type-I vertex addition, where $\mathcal{N}_i$ denotes agent i's sensing neighbor set. Following Proposition 1 (case 2), we first introduce a constructive mechanism for building an N-agent globally angle rigid formation by Type-I vertex addition. Denote by $\alpha^*_{jik} \in (0, \pi)$ agent i's desired angle formed with agents j, k.

Algorithm 1: Construct An N-Agent Globally Angle Rigid Formation Based on Type-I Vertex Addition (Case 2).

Step 1: Construct the first triangular formation using three desired interior angles $\alpha^*_{312}, \alpha^*_{123}, \alpha^*_{231}$.

Step 2: Add agent 4 using three desired interior angles $\alpha^*_{412}, \alpha^*_{421}, \alpha^*_{423}$ and one desired counterclockwise constraint of agent 4 with respect to agents 1, 2, 3.

...

Step k-2: Add agent k using three desired interior angles $\alpha^*_{ki_1i_2}, \alpha^*_{ki_2i_1}, \alpha^*_{ki_2i_3}, i_1 < k, i_2 < k, i_3 < k$ and one desired counterclockwise constraint of agent k with respect to agents i_1, i_2, i_3.

...

Step N-2: Add agent N using three desired interior angles $\alpha^*_{Nj_1j_2}, \alpha^*_{Nj_2j_1}, \alpha^*_{Nj_2j_3}, j_1 < N, j_2 < N, j_3 < N$ and one desired counterclockwise constraint of agent N with respect to agents j_1, j_2, j_3.

Similarly, a mechanism based on the Type-II vertex addition can also be proposed to construct an N-agent angle rigid formation. Correspondingly, in the follow-up sections, we first control the first three agents to form the desired triangular formation, and then control the remaining agents following the sequence of Type-I or Type-II vertex additions. Finally, we consider the control of convex polyhedral formations.

A. Formation Control for the First Three Agents

In this section, the control objectives for agents 1 to 3 are

$$\lim_{t\to\infty} e_i(t) = \lim_{t\to\infty} \left(\alpha_{[i-1]i[i+1]}(t) - \alpha^*_{[i-1]i[i+1]}\right) = 0 \tag{3}$$

where $i = 1, 2, 3$, $[i] = i$ for $i = 1, .., 3$, $[i-1] = 3$ for $i = 1$, $[i+1] = 1$ for $i = 3$, and $\alpha_{jik} = \arccos\left(b_{ij}^{\mathrm{T}} b_{ik}\right)$. Different from the bisector moving rule employed for 2-D angle rigid formations [14], motivated by [37], we design the following cyclic pursuing rule:

$$u_i(t) = -\left(\alpha_{[i-1]i[i+1]}(t) - \alpha^*_{[i-1]i[i+1]}\right) b_{i[i+1]}(t) \tag{4}$$

where each agent i only needs to measure the directions $\overrightarrow{i[i+1]}$ and $\overrightarrow{i[i-1]}$ in its own coordinate frame to implement (4), and no interagent communication is required. Now, we study the angle error dynamics. Suppose $l_{ij}(0) \neq 0$ and $\sin\alpha_{jik}(0) \neq 0, i, j, k = 1, 2, 3$, then $\exists T_1 > 0$ such that $l_{ij}(t) \neq 0, \sin\alpha_{jik}(t) \neq 0, \forall t \in [0, T_1)$. Then for $t \in [0, T_1)$, according to the calculation of an angle's time-derivative in [38, Eq. (6)] or [14, Eq. (31)], one has

$$\begin{aligned}\dot{e}_1 = \dot{\alpha}_{312} &= -\left(\dot{b}_{13}^{\mathrm{T}} b_{12} + b_{13}^{\mathrm{T}} \dot{b}_{12}\right) / \sin\alpha_{312} \\ &= -\left[\frac{P_{b_{13}}(\dot{p}_3 - \dot{p}_1)}{l_{13}\sin\alpha_{312}}\right]^{\mathrm{T}} b_{12} - b_{13}^{\mathrm{T}} \frac{P_{b_{12}}(\dot{p}_2 - \dot{p}_1)}{l_{12}\sin\alpha_{312}}.\end{aligned} \tag{5}$$

where $P_{b_{13}} = I_3 - b_{13} b_{13}^{\top}$. By substituting (4) into (5), it follows:

$$\begin{aligned}b_{13}^{\mathrm{T}} \dot{b}_{12} &= b_{13}^{\mathrm{T}} P_{b_{12}} / l_{12} \left[\left(\alpha_{312} - \alpha^*_{312}\right) b_{12} - \left(\alpha_{123} - \alpha^*_{123}\right) b_{23}\right] \\ &= -\left(\sin\alpha_{312}\sin\alpha_{123}/l_{12}\right)\left(\alpha_{123} - \alpha^*_{123}\right).\end{aligned} \tag{6}$$

Similarly

$$\dot{b}_{13}^{\mathrm{T}} b_{12} = \left(b_{12}^{\mathrm{T}} P_{b_{13}}/l_{13}\right)\left[(\alpha_{312}-\alpha_{312}^*)b_{12}-(\alpha_{231}-\alpha_{231}^*)b_{31}\right] = \left(\sin^2\alpha_{312}/l_{13}\right)(\alpha_{312}-\alpha_{312}^*). \quad (7)$$

By substituting (6) and (7) into (5), one obtains

$$\dot{e}_1 = -(\sin\alpha_{312}/l_{13})e_1 + (\sin\alpha_{123}/l_{12})e_2. \quad (8)$$

By following the steps similar to (5)–(8), one has the dynamics $\dot{e}_2$ and $\dot{e}_3$. Then, one has the overall angle error dynamics of the first three agents

$$\dot{e}_f = \begin{bmatrix}\dot{e}_1\\ \dot{e}_2\\ \dot{e}_3\end{bmatrix} = F_1(e_f)e_f = \begin{bmatrix}-g_{312} & g_{123} & 0\\ 0 & -g_{123} & g_{231}\\ g_{312} & 0 & -g_{231}\end{bmatrix} e_f \quad (9)$$

where $g_{jik} = \sin\alpha_{jik}/l_{ji}, i,j,k \in \{1,2,3\}$. Since $e_1+e_2+e_3 \equiv 0$, e_1, e_2, e_3 are linearly dependent. Using the fact $\dot{e}_2 = -g_{123}e_2 + g_{231}e_3 = -g_{231}e_1 - (g_{123}+g_{231})e_2$, (9) can be equivalently described by

$$\dot{e}_s = \begin{bmatrix}\dot{e}_1\\ \dot{e}_2\end{bmatrix} = \begin{bmatrix}-g_{312} & g_{123}\\ -g_{231} & -(g_{123}+g_{231})\end{bmatrix}\begin{bmatrix}e_1\\ e_2\end{bmatrix} = F_s(e_s)e_s. \quad (10)$$

Although (10) is derived for $t \in [0, T_1)$, we now show that T_1 can be extended to infinity.

Lemma 8 (Noncollinearity): For the three-agent formation under the control law (4), if the formation is not initially collinear, it will not become collinear for $\forall t > 0$, and thus (10) applies for any $t > 0$.

Proof: We prove by contradiction. Suppose collinearity may occur for $t > T_1$, and let T_s be the first time at which the three agents approach being collinear. Then at T_s^-, it must be true that for the triangular formation formed by these three agents, two interior angles approach zero and the third approaches π. Without loss of generality, assume that agent 1 is the agent associated with the interior angle approaching π, and thus $\alpha_1(T_s^-) = \pi - \epsilon_1$, $\alpha_2(T_s^-) = \epsilon_2$ and $\alpha_3(T_s^-) = \epsilon_3$ for some infinitesimally small positive numbers ϵ_1, ϵ_2, and ϵ_3 satisfying $\epsilon_1 = \epsilon_2 + \epsilon_3$. For $t \in [0, T_s)$, one has

$$\dot{e}_1 = -g_{312}e_1 + g_{123}e_2. \quad (11)$$

Since α_1^* is bounded away from π, $e_1(T_s^-) > 0$; since α_2^* is bounded away from zero, $e_2(T_s^-) < 0$. In addition, one can further check that at T_s^-, $g_{312} > 0$ and $g_{123} > 0$. Hence, $\dot{e}_1(T_s^-) < 0$, which implies that at T_s^-, if time further evolves, α_1 decreases away from π, which contradicts the assumption that at T_s, the three agents become collinear and thus α_1 becomes π. This contradiction completes the proof. □

Now, we present the convergence result for the three agents.

Theorem 4: For the three-agent formation under the control law (4), if $\alpha_{312}(0), \alpha_{123}(0), \alpha_{231}(0)$ are not zero, the initial angle errors $e_i(0), i = 1,2,3$ are sufficiently small and the initial distances $l_{12}(0), l_{23}(0), l_{31}(0)$ are bounded away from zero, then the angle errors $e_i(t)$ converge exponentially to zero.

Proof: To show the local convergence of e_i, we use linearization to analyze the angle error dynamics (10). By taking e_1 as an example, the linearized dynamics around the desired equilibrium $e_s = 0$ are

$$\dot{e}_1 = \left[\frac{\partial(-g_{312}e_1 + g_{123}e_2)}{\partial e_1}|_{e_s=0}\right] e_1 + \left[\frac{\partial(-g_{312}e_1 + g_{123}e_2)}{\partial e_2}|_{e_s=0}\right] e_2 = -g_{312}^* e_1 + g_{123}^* e_2 \quad (12)$$

where $g_{jik}^* = g_{jik}|_{e_s=0}, j \neq i \neq k$ and $j,i,k \in \{1,2,3\}$. Then, by following the same step as (12) for e_2, the linearized dynamics of (10) can be written as

$$\dot{e}_s = A_1 e_s \quad (13)$$

where $A_1 = F_s(e_s)|_{e_s=0}$ is a 2-by-2 constant matrix. Then, one has $\mathrm{tr}(A_1) = -g_{312}^* - g_{123}^* - g_{231}^* < 0$ and $\det(A_1) = g_{312}^*(g_{123}^* + g_{231}^*) + g_{123}^* g_{231}^* > 0$, where tr() and det() represent the trace and determinant of a square matrix, respectively. It follows that A_1 is Hurwitz. Following [14, Th. 5], it is straightforward to have that

$$e_1^2 + e_2^2 = \|e_s\|^2 \leq \frac{V_1}{\lambda_{\min}(P_1)} \leq \frac{V_1(0)}{\lambda_{\min}(P_1)} e^{-\frac{t}{\lambda_{\max}(P_1)}}. \quad (14)$$

where $V_1 = e_s^{\mathrm{T}} P_1 e_s$ and $-I_2 = P_1 A_1 + A_1^{\mathrm{T}} P_1$. Since $e_1 + e_2 + e_3 \equiv 0$, one has

$$e_3^2 = e_1^2 + e_2^2 + 2e_1e_2 \leq 2\left(e_1^2 + e_2^2\right) \leq \frac{2\,V_1(0)}{\lambda_{\min}(P_1)} e^{-\frac{t}{\lambda_{\max}(P_1)}}$$

which implies that $e_i, i = 1,2,3$, under the dynamics (9) is locally and exponentially stable. □

Remark 5: The triangular formation's local convergence is still guaranteed if the control law (4) is generalized to $u_i(t) = -(\alpha_{[i-1]i[i+1]}(t) - \alpha_{[i-1]i[i+1]}^*)(\gamma_1 b_{i[i-1]}(t) + \gamma_2 b_{i[i+1]}(t))$, where $\gamma_1 \geq 0, \gamma_2 \geq 0$ and $\gamma_1 + \gamma_2 = 1$. The stability analysis for the cases $\gamma_1 = 0$ and $\gamma_1 = 1$ is given in Theorem 4. For the case $\gamma_1 \in (0,1)$, where each agent moves towards the inner side of its interior angle (or its opposite direction), since $u_1(t), u_2(t), u_3(t)$ always lie in the plane formed by $p_1(0), p_2(0), p_3(0)$, the evolution trajectories of the first three agents will be within a 2-D plane. According to [39], the stability under $\gamma_1 \in (0,1)$ can be obtained straightforwardly. Combining the above two cases, one has that a convex combination of $b_{i[i-1]}$ and $b_{i[i+1]}$ in agent i's controller is valid for the formation's convergence.

Since the convergence of (10) is only proved to be local, we now propose another control strategy such that the triangular formation is (almost) globally stable. Consider that agent 1 is static, i.e., $\dot{p}_1(t) = 0$, and agents 2 and 3 are controlled by

$$u_2 = -(\alpha_{123} - \alpha_{123}^*)\, b_{23}, \quad u_3 = -(\alpha_{231} - \alpha_{231}^*)\, b_{32} \quad (15)$$

where no interagent communication is required.

Theorem 5: For the three-agent formation under the control laws (15), if $p_1(0), p_2(0), p_3(0)$ are not collinear, then the angle errors $e_i(t), i = 1,2,3$ globally converge to zero.

Proof: According to the moving directions of agents 2 and 3, the three agents will not be collinear for $\forall t > 0$. Now, we first prove that no collision will occur between agents 2 and 3 using contradiction. Suppose that agents 2 and 3 first collide at $t = T_c > 0$. Then, there are three possible cases for the two agents' status at T_c^-, namely, (a) one of them is static, (b) they move

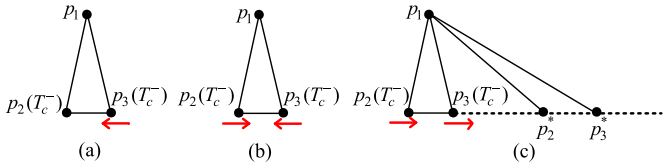

Fig. 9. Three possible collision cases.

toward each other, (c) they move along the same direction, which are shown in Fig. 9. For the case (a), agent 2 being static implies $\alpha_{123}(T_c^-) = \alpha_{123}^*$. Since the angle α_{132} decreases monotonically along the ray $\overrightarrow{23}$, there exists a unique position p_3^* in $\overrightarrow{23}$ such that $\alpha_{231}(p_2(T_c^-), p_3^*, p_1) = \alpha_{231}^*$. Since p_3^* is bounded away from $p_2(T_c^-)$ and agent 3 is controlled by an angle error feedback law (15), it is impossible that agent 3 will collide with agent 2 at $p_2(T_c^-)$. For case (b), according to the moving directions of the agents, $\alpha_{123}(T_c^-) < \alpha_{123}^*$ and $\alpha_{231}(T_c^-) < \alpha_{231}^*$. Then, the fact that $\alpha_{123}(T_c^-) + \alpha_{132}(T_c^-)$ is sufficiently close to π contradicts the fact that $\pi = \alpha_{123}^* + \alpha_{231}^* + \alpha_{312}^* > \alpha_{123}(T_c^-) + \alpha_{231}(T_c^-) + \alpha_{312}^*$ since α_{312}^* is bounded away from 0. For case (c), denote by p_2^*, p_3^* the desired positions of agents 2, 3, respectively. According to the agents' moving directions, p_3^* must be in the right side of p_2^* and $\|u_2(T_c^-)\| = |e_2(T_c^-)| > \|u_3(T_c^-)\| = |e_3(T_c^-)|$. Since $\alpha_{123}^* = \alpha_{212}(p_2^*, p_1, p_2(T_c^-)) + \alpha_{123}(T_c^-)$ and $\alpha_{132}(T_c^-) = \alpha_{132}^* + \alpha_{313}(p_3(T_c^-), p_1, p_3^*)$, one has $|e_2(T_c^-)| = \alpha_{212}(p_2^*, p_1, p_2(T_c^-))$ and $|e_3(T_c^-)| = \alpha_{313}(p_3(T_c^-), p_1, p_3^*)$. Since $p_2(T_c^-)$ is sufficiently close to $p_3(T_c^-)$ and p_2^* is bounded away from p_3^*, $\alpha_{212}(p_2^*, p_1, p_2(T_c^-)) < \alpha_{313}(p_3(T_c^-), p_1, p_3^*)$ which contradicts the fact $|e_2(T_c^-)| > |e_3(T_c^-)|$. Since these three cases are impossible, $l_{23}(t)$ is bounded away from zero $\forall t > 0$, which also implies $\sin\alpha_{123}(t), \sin\alpha_{231}(t)$ are bounded away from zero. Then, following (5), one has the overall angle error dynamics:

$$\begin{bmatrix} \dot{e}_2 \\ \dot{e}_3 \end{bmatrix} = -\begin{bmatrix} \sin\alpha_{123}/l_{21} & 0 \\ 0 & \sin\alpha_{231}/l_{31} \end{bmatrix} \begin{bmatrix} \alpha_{123} - \alpha_{123}^* \\ \alpha_{231} - \alpha_{231}^* \end{bmatrix} \tag{16}$$

Since $\sin\alpha_{123}/l_{21} > 0$ and $\sin\alpha_{231}/l_{31} > 0$ are lower and upper bounded, e_2, e_3 converge to zero globally according to [40, Th. 2.5.1]. □

B. Sequential Formation Control for the Remaining Agents by Type-I Vertex Addition

In this section, we control the remaining agents to achieve their desired angles defined in the constructive Algorithm 1's Steps 2 to $N-2$. To be specific, the control objectives for agent $i, 4 \le i \le N$, are

$$\lim_{t\to\infty} e_{i1}(t) = \lim_{t\to\infty} \left(\alpha_{ij_1j_2}(t) - \alpha_{ij_1j_2}^*\right) = 0 \tag{17}$$

$$\lim_{t\to\infty} e_{i2}(t) = \lim_{t\to\infty} \left(\alpha_{ij_2j_1}(t) - \alpha_{ij_2j_1}^*\right) = 0 \tag{18}$$

$$\lim_{t\to\infty} e_{i3}(t) = \lim_{t\to\infty} \left(\alpha_{ij_2j_3}(t) - \alpha_{ij_2j_3}^*\right) = 0 \tag{19}$$

where $i = 4, \ldots, N$, $j_1 \ne j_2 \ne j_3$ $j_1 < i, j_2 < i, j_3 < i$, and $\alpha_{ij_1j_2}^* \in (0, \pi), \alpha_{ij_2j_1}^* \in (0, \pi), \alpha_{ij_2j_3}^* \in (0, \pi)$ denote three desired angles that agent i aims at maintaining with its neighboring agents j_1, j_2, j_3.

We first illustrate how to control agent 4, and then extend the result to the N-agent case. We propose the following control law for agent 4

$$\begin{aligned} u_4 = {} & (\alpha_{412} - \alpha_{412}^*)\, b_{42} + (\alpha_{421} - \alpha_{421}^*)\, b_{41} \\ & + (\alpha_{423} - \alpha_{423}^*)\, b_{43}. \end{aligned} \tag{20}$$

where the real-time angle information $\alpha_{412} = \arccos\left(b_{14}^{\mathrm{T}} b_{12}\right)$ cannot be calculated by agent 4's own direction measurements, but can be calculated via agent 1's direction measurements $\overrightarrow{14}, \overrightarrow{12}$. Therefore, the implementation of control law (20) relies on not only agent 4's direction measurements $\overrightarrow{41}, \overrightarrow{42}, \overrightarrow{43}$, but also the real-time angle information $\alpha_{412}(t), \alpha_{421}(t), \alpha_{423}(t)$ which can be sent from agents 1 and 2 to agent 4 through wireless communication. Now, we present the convergence of agent 4.

Theorem 6: For the four-agent formation under the control (4) and (20), if $\alpha_{123}(0), \alpha_{231}(0), \alpha_{312}(0), \alpha_{412}(0), \alpha_{421}(0), \alpha_{423}(0)$ are not zero or π, the initial angle errors $e_i(0), e_{4i}(0), i = 1, 2, 3$ are sufficiently small, the initial distances $l_{jk}(0), j \ne k, j, k \in \{1, 2, 3, 4\}$ are bounded away from zero and $p_4(0)$ is sufficiently away from the plane formed by $p_1(0), p_2(0), p_3(0)$, then the angle errors $e_{4i}(t)$ converge exponentially to zero.

Proof: Since $l_{jk}(0)$ and $\sin\alpha_{412}(0), \sin\alpha_{421}(0), \sin\alpha_{423}(0)$ are not zero, $\exists T_2 > 0$ such that for $t \in [0, T_2)$, $l_{jk}(t) \ne 0$ and $\sin\alpha_{412}(t), \sin\alpha_{421}(t), \sin\alpha_{423}(t)$ are not zero. Now, we study the dynamics of angle errors $e_{41} = \alpha_{412} - \alpha_{412}^*$, $e_{42} = \alpha_{421} - \alpha_{421}^*$, $e_{43} = \alpha_{423} - \alpha_{423}^*$. Taking e_{41} as an example, similar to (5), one has

$$\dot{e}_{41} = -\left[\frac{P_{b_{14}}(\dot{p}_4 - \dot{p}_1)}{l_{14}\sin\alpha_{412}}\right]^{\mathrm{T}} b_{12} - b_{14}^{\mathrm{T}} \frac{P_{b_{12}}(\dot{p}_2 - \dot{p}_1)}{l_{12}\sin\alpha_{412}}. \tag{21}$$

Substituting (20) and (4) into (21) yields

$$\begin{aligned} \dot{e}_{41} = {} & -\frac{\sin\alpha_{142}}{l_{14}}(\alpha_{412} - \alpha_{412}^*) - \frac{b_{12}^{\mathrm{T}} P_{b_{14}} b_{43}}{l_{14}\sin\alpha_{412}}(\alpha_{423} - \alpha_{423}^*) \\ & - e_1 b_{12}^{\mathrm{T}} P_{b_{14}} b_{12}/(l_{14}\sin\alpha_{412}) \\ & + e_2 b_{14}^{\mathrm{T}} P_{b_{12}} b_{23}/(l_{12}\sin\alpha_{412}). \end{aligned}$$

Similarly, one can compute $\dot{e}_{42}$ and $\dot{e}_{43}$ to obtain

$$\begin{aligned} \dot{e}_4 = {} & \begin{bmatrix} \dot{e}_{41} & \dot{e}_{42} & \dot{e}_{43} \end{bmatrix}^{\mathrm{T}} = F_4(e_s, e_4)e_4 + G_4(e_s, e_4)e_s \\ = {} & -\begin{bmatrix} \frac{\sin\alpha_{142}}{l_{14}} & 0 & \frac{b_{12}^{\mathrm{T}} P_{b_{14}} b_{43}}{l_{14}\sin\alpha_{412}} \\ 0 & \frac{\sin\alpha_{142}}{l_{24}} & \frac{b_{21}^{\mathrm{T}} P_{b_{24}} b_{43}}{l_{24}\sin\alpha_{421}} \\ 0 & \frac{b_{23}^{\mathrm{T}} P_{b_{24}} b_{41}}{l_{24}\sin\alpha_{423}} & \frac{\sin\alpha_{243}}{l_{24}} \end{bmatrix} \begin{bmatrix} e_{41} \\ e_{42} \\ e_{43} \end{bmatrix} \\ & + \begin{bmatrix} G_{11} & G_{12} \\ G_{21} & G_{22} \\ G_{31} & G_{32} \end{bmatrix} \begin{bmatrix} e_1 \\ e_2 \end{bmatrix} \end{aligned} \tag{22}$$

where $G_{11} = -\frac{b_{12}^{\mathrm{T}} P_{b_{14}} b_{12}}{l_{41}\sin\alpha_{412}}$, $G_{12} = \frac{b_{14}^{\mathrm{T}} P_{b_{12}} b_{23}}{l_{12}\sin\alpha_{412}}$, $G_{21} = 0$, $G_{22} = -\left(\frac{b_{21}^{\mathrm{T}} P_{b_{24}} b_{23}}{l_{24}\sin\alpha_{421}} + \frac{b_{24}^{\mathrm{T}} P_{b_{21}} b_{23}}{l_{21}\sin\alpha_{421}}\right)$, $G_{31} = -\frac{b_{24}^{\mathrm{T}} P_{b_{23}} b_{31}}{l_{23}\sin\alpha_{423}}$, $G_{32} = -\left(\frac{b_{23}^{\mathrm{T}} P_{b_{24}} b_{23}}{l_{24}\sin\alpha_{423}} + \frac{b_{24}^{\mathrm{T}} P_{b_{23}} b_{31}}{l_{23}\sin\alpha_{423}}\right)$. Then, we check the local stability of the four-agent formation. Linearizing (22) around the desired equilibrium $\{e_s = 0, e_4 = 0\}$ by following (12),

one has the linearized dynamics

$$\dot{e}_4 = A_4 e_4 + B_4 e_s \tag{23}$$

where $A_4 = F_4(e_s, e_4)|_{e_s=0,e_4=0}$, $B_4 = G_4(e_s, e_4)|_{e_s=0,e_4=0}$ are constant matrices. Now, we check whether A_4 is Hurwitz.

$$\begin{aligned}&\det(\lambda I_3 - A_4)\\ &= (\lambda + \sin\alpha^*_{142}/l^*_{14})\,(\lambda + \sin\alpha^*_{142}/l^*_{24})\,(\lambda + \sin\alpha^*_{243}/l^*_{24})\\ &\quad - \left(\lambda + \frac{\sin\alpha^*_{142}}{l^*_{14}}\right)\frac{(b^{*\mathrm{T}}_{21} P_{b^*_{24}} b^*_{43})}{l^*_{24}\sin\alpha^*_{421}}\,\frac{(b^{*\mathrm{T}}_{23} P_{b^*_{24}} b^*_{41})}{l^*_{24}\sin\alpha^*_{423}}\end{aligned} \tag{24}$$

where $\lambda \in \mathbb{C}$ denotes the eigenvalue of A_4, l^*_{ji} and b^*_{ji}, $j, i \in \mathcal{V}$ are the distance and bearing evaluated at $\{e_s = 0, e_4 = 0\}$, respectively. Checking the eigenvalues of A_4 by letting $\det(\lambda I_3 - A_4) = 0$, one has that A_4 always has an eigenvalue $-\sin\alpha^*_{142}/l^*_{14} < 0$. However, due to the second component in (24), it is challenging to check the sign of the real parts of the remaining two eigenvalues of A_4. Here, we first calculate

$$\begin{aligned}&(b^{*\mathrm{T}}_{21} P_{b^*_{24}} b^*_{43})\,(b^{*\mathrm{T}}_{23} P_{b^*_{24}} b^*_{41})\\ &= (l^*_{23} b^{*\mathrm{T}}_{21} P_{b^*_{24}} b^*_{23}/l^*_{43})\,(l^*_{43} b^{*\mathrm{T}}_{43} P_{b^*_{24}} b^*_{41}/l^*_{23})\\ &= [\cos\alpha^*_{123} - \cos\alpha^*_{423}\cos\alpha^*_{421}]\,[\cos\alpha^*_{143}\\ &\quad - \cos\alpha^*_{142}\cos\alpha^*_{243}]\end{aligned} \tag{25}$$

where we used the facts that $b_{43} = \frac{(p_3 - p_2) + (p_2 - p_4)}{l_{43}}$, $P_{b_{24}}(p_2 - p_4) = 0$, and $b_{23} = \frac{(p_3 - p_4) + (p_4 - p_2)}{l_{23}}$. Then, the other two eigenvalues of A_4 satisfy

$$\lambda^2 + (\sin\alpha^*_{142}/l^*_{24} + \sin\alpha^*_{243}/l^*_{24})\,\lambda + \varepsilon_1 = 0 \tag{26}$$

where $\varepsilon_1 = -\frac{[\cos\alpha^*_{123} - \cos\alpha^*_{423}\cos\alpha^*_{421}]}{l^*_{24}\sin\alpha^*_{421}}\,\frac{[\cos\alpha^*_{143} - \cos\alpha^*_{142}\cos\alpha^*_{243}]}{l^*_{24}\sin\alpha^*_{423}} + \frac{\sin\alpha^*_{142}}{l^*_{24}}\,\frac{\sin\alpha^*_{243}}{l^*_{24}}$. If $\varepsilon_1 > 0$, then the remaining two eigenvalues of A_4 have negative real parts, which implies that A_4 is Hurwitz. Note that $\varepsilon_1 > 0$ is equivalent to

$$\begin{aligned}&\sin\alpha^*_{421}\sin\alpha^*_{423}\sin\alpha^*_{142}\sin\alpha^*_{243}\\ &> [\cos\alpha^*_{123} - \cos\alpha^*_{423}\cos\alpha^*_{421}][\cos\alpha^*_{143} - \cos\alpha^*_{142}\cos\alpha^*_{243}].\end{aligned} \tag{27}$$

Now, we prove that (27) holds for all tetrahedral formations formed by agents 1–4. Splitting (27) into two inequalities $\sin\alpha^*_{421}\sin\alpha^*_{423} > |\cos\alpha^*_{123} - \cos\alpha^*_{423}\cos\alpha^*_{421}|$ and $\sin\alpha^*_{142}\sin\alpha^*_{243} > |\cos\alpha^*_{143} - \cos\alpha^*_{142}\cos\alpha^*_{243}|$, we first illustrate how to prove the first inequality by using the facts that $\alpha^*_{123} \in (0, \pi), \alpha^*_{423} \in (0, \pi), \alpha^*_{421} \in (0, \pi)$, and $\alpha^*_{123} + \alpha^*_{423} + \alpha^*_{421} < 2\pi$, $2\pi > \alpha^*_{ijk} + \alpha^*_{ijm} > \alpha^*_{kjm} > 0, i, j, k, m \in \{1, 2, 3, 4\}$. There are three possible cases.

Case 1: $\cos\alpha^*_{123} > \cos\alpha^*_{423}\cos\alpha^*_{421}$. When $\alpha^*_{423} \le \alpha^*_{421}$, by using $0 < \alpha^*_{421} < \alpha^*_{123} + \alpha^*_{423}$, one has that $0 \le \alpha^*_{421} - \alpha^*_{423} < \alpha^*_{123} < \pi$. It follows that $\cos(\alpha^*_{421} - \alpha^*_{423}) > \cos\alpha^*_{123}$, which gives $\sin\alpha^*_{421}\sin\alpha^*_{423} > \cos\alpha^*_{123} - \cos\alpha^*_{423}\cos\alpha^*_{421}$. When $\alpha^*_{423} > \alpha^*_{421}$, by using $\alpha^*_{423} < \alpha^*_{421} + \alpha^*_{123}$, one has $-\pi < -\alpha^*_{123} < \alpha^*_{421} - \alpha^*_{423} < 0$. It follows that $\cos(\alpha^*_{421} - \alpha^*_{423}) > \cos(-\alpha^*_{123}) = \cos(\alpha^*_{123})$, which also gives $\sin\alpha^*_{421}\sin\alpha^*_{423} > \cos\alpha^*_{123} - \cos\alpha^*_{423}\cos\alpha^*_{421}$.

Case 2: $\cos\alpha^*_{123} < \cos\alpha^*_{423}\cos\alpha^*_{421}$. When $\pi \le \alpha^*_{421} + \alpha^*_{423} < 2\pi$, by using $\alpha^*_{123} \in (0, \pi)$, $(2\pi - (\alpha^*_{421} + \alpha^*_{243})) \in (0, \pi]$ and $\alpha^*_{123} < 2\pi - (\alpha^*_{421} + \alpha^*_{423})$, one has $\cos\alpha^*_{123} > \cos(2\pi - (\alpha^*_{421} + \alpha^*_{423})) = \cos(\alpha^*_{421} + \alpha^*_{423})$. It follows $\sin\alpha^*_{421}\sin\alpha^*_{423} > \cos\alpha^*_{423}\cos\alpha^*_{421} - \cos\alpha^*_{123}$. When $0 < \alpha^*_{421} + \alpha^*_{423} \le \pi$, by using $0 < \alpha^*_{123} < \alpha^*_{421} + \alpha^*_{423} \le \pi$, one also has $\sin\alpha^*_{421}\sin\alpha^*_{423} > \cos\alpha^*_{423}\cos\alpha^*_{421} - \cos\alpha^*_{123}$.

Case 3: $\cos\alpha^*_{123} = \cos\alpha^*_{423}\cos\alpha^*_{421}$. This case is obvious.

Combining the above three cases together, one has that $\sin\alpha^*_{421}\sin\alpha^*_{423} > |\cos\alpha^*_{123} - \cos\alpha^*_{423}\cos\alpha^*_{421}|$ holds for all tetrahedral formations. The same analysis can be conducted for the second inequality, which proves (27).

By combining (25)–(27), one has that A_4 is always Hurwitz for tetrahedral formations formed by agents 1–4. Writing (13) and (23) into a compact form yields

$$\dot{\bar{e}}_4 = \begin{bmatrix}\dot{e}_s\\ \dot{e}_4\end{bmatrix} = H_4 \bar{e}_4 = \begin{bmatrix}A_1 & 0\\ B_4 & A_4\end{bmatrix}\begin{bmatrix}e_s\\ e_4\end{bmatrix}. \tag{28}$$

Because A_1 and A_4 are Hurwitz, H_4 is also Hurwitz. Then, for the identity matrix $I_5 \in \mathbb{R}^{5\times 5}$, there exists a positive definite matrix $P_2 \in \mathbb{R}^{5\times 5}$ such that $P_2 H_4 + H_4^{\mathrm{T}} P_2 = -I_5$. Construct the Lyapunov function

$$V_2 = \bar{e}_4^{\mathrm{T}} P_2 \bar{e}_4. \tag{29}$$

Taking the time-derivative of (29) yields $\dot{V}_2 = -\bar{e}_4^{\mathrm{T}}\bar{e}_4 \le -V_2/\lambda_{\max}(P_2)$, which implies that

$$\|e_4\|^2 \le \|\bar{e}_4\|^2 \le \frac{V_2}{\lambda_{\min}(P_2)} \le \frac{V_2(0)}{\lambda_{\min}(P_2)} e^{-\frac{t}{\lambda_{\max}(P_2)}} \tag{30}$$

which implies the exponential stability of $\|e_4(t)\|$ for $t \in [0, T_2)$. Since $\|\dot{p}_4\| \le |e_{41}| + |e_{42}| + |e_{43}| \le \sqrt{3}\|e_4\| \le \sqrt{\frac{3V_2(0)}{\lambda_{\min}(P_2)}} e^{-\frac{t}{2\lambda_{\max}(P_2)}}$, one has $\|p_4(t) - p_4(0)\| \le \int_0^t \|\dot{p}_4(\tau)\| d\tau \le 2\lambda_{\max}(P_2)\sqrt{\frac{3V_2(0)}{\lambda_{\min}(P_2)}}(1 - e^{-\frac{t}{2\lambda_{\max}(P_2)}})$ for $t \in [0, T_2)$. Since $V_2(0)$ is sufficiently small, $\|p_4(t) - p_4(0)\|$ is also sufficiently small for $t \in [0, T_2)$. Since $p_4(0)$ is sufficiently away from the plane formed by $p_1(0), p_2(0), p_3(0)$, $p_4(T_2^-)$ is also sufficiently away from the plane formed by $p_1(0), p_2(0), p_3(0)$, which implies that $l_{4i}(T_2^-), i = 1, 2, 3$ and $\sin\alpha_{412}(T_2^-), \sin\alpha_{421}(T_2^-), \sin\alpha_{423}(T_2^-)$ are not zero. Then, one can extend T_2^- to T_3, $T_3 > T_2$. In fact one can check that when $T_3 \to \infty$, $\|p_4(t) - p_4(0)\|$ is still sufficiently small for $\forall t \in [0, \infty)$, which implies that (22) is always well-defined and $\|e_4(t)\|$ is exponentially stable for $\forall t \in [0, \infty)$. □

Remark 6: The first three agents always lie in the plane formed by $p_1(0), p_2(0), p_3(0)$ since the control actions (4) are confined in this plane. If $\exists T_3$ such that $p_4(T_3)$ lies in that plane, then $p_4(t), \forall t > T_3$ will always be in that plane according to the control law (20). Then, the angle error (22) will not converge to zero because in this case $F_4(e_s, e_4)$ becomes singular. Therefore, Theorem 6 requires that $p_4(0)$ is sufficiently away from the plane formed by $p_1(0), p_2(0), p_3(0)$.

Now, we precisely describe the requirements on $l_{4i}(0), i = 1, 2, 3$, $e_{4i}(0)$ and the initial distance $h_{4-123}(0)$ between $p_4(0)$ and the plane formed by $p_1(0), p_2(0), p_3(0)$ such that (22) is well-defined. First, taking l_{41} as an example and letting the first three agents static, one has

$$l_{41}(t) = l_{41}(0) + \int_0^t \dot{l}_{41} d\tau \ge l_{41}(0) - \int_0^t |b_{41}^{\mathrm{T}}(\dot{p}_1 - \dot{p}_4)| d\tau$$

$$\geq l_{41}(0) - 4\sqrt{\frac{V_2(0)}{\lambda_{\min}(P_2)}}\lambda_{\max}(P_2)\left(1 - e^{-\frac{t}{2\lambda_{\max}(P_2)}}\right) \tag{31}$$

which implies that if $l_{41}(0) > 4\sqrt{V_2(0)/\lambda_{\min}(P_2)}\lambda_{\max}(P_2)$, then no collision between agents 1 and 4 will occur for $t > 0$.

To guarantee that $1/\sin\alpha_{412}$ is well-defined in (21), one requires $0 < \alpha_{412}(t) < \pi$. According to (30), one has

$$|e_{41}| = |\alpha_{412} - \alpha^*_{412}| \leq \|e_4\| \leq \sqrt{V_2(0)/\lambda_{\min}(P_2)}. \tag{32}$$

It follows that $\alpha^*_{412} - \sqrt{V_2(0)/\lambda_{\min}(P_2)} \leq \alpha_{412}(t) \leq \alpha^*_{412} + \sqrt{V_2(0)/\lambda_{\min}(P_2)}$. Therefore, if $\sqrt{V_2(0)} < \sqrt{\lambda_{\min}(P_2)} * \min\{\pi - \alpha^*_{412}, \alpha^*_{412}\}$, one always has $0 < \alpha_{412}(t) < \pi$.

The distance $h_{4-123}(t)$ between $p_4(t)$ and the plane formed by $p_1(0), p_2(0), p_3(0)$ can be calculated by $h_{4-123}(t) = \frac{V_{4-123}}{S_{123}(0)} = \frac{p^{\mathrm{T}}_{4\bar{1}}(t)(p_{4\bar{2}}(t)\times p_{4\bar{3}}(t))}{3l_{12}(0)l_{13}(0)\sin\alpha_{213}(0)}$, where $p_{4\bar{i}}(t) = p_i(0) - p_4(t), i = 1, 2, 3$. Then, one has

$$\dot{V}_{4-123} = \frac{1}{6}\dot{p}^{\mathrm{T}}_4\left(p_{4\bar{2}} \times p_{4\bar{3}}\right) + p^{\mathrm{T}}_{4\bar{1}}\left[\dot{p}_4 \times (p_3(0) - p_2(0))\right]$$

$$\leq \frac{1}{6}\left(|e_{41}| + |e_{42}| + |e_{43}|\right)\left[l_{42(\max)}l_{43(\max)} + l_{32}(0)l_{41(\max)}\right]$$

where $l_{4i(\max)} = \max\{\|p_{4\bar{i}}(t)\|, \forall t > 0\} = l_{4i}(0) + 4\sqrt{V_2(0)/\lambda_{\min}(P_2)}\lambda_{\max}(P_2)$, and we used the fact $\|p_{4\bar{i}}(t)\| \leq l_{4i}(0) + \int_0^t \|\dot{p}_4(\tau)\|d\tau \leq l_{4i}(0) + \int_0^t(|e_{41}| + |e_{42}| + |e_{43}|)\|d\tau \leq l_{4i}(0) + 4\sqrt{V_2(0)/\lambda_{\min}(P_2)}\lambda_{\max}(P_2)$. Therefore, one has

$$h_{4-123}(t) \geq h_{4-123}(0) - \int_0^t |\dot{V}_{4-123}(\tau)|/S_{123}(0)d\tau$$

$$\geq h_{4-123}(0) - \varepsilon_2\left(1 - e^{-0.5t/\lambda_{\max}(P_2)}\right) \tag{33}$$

where $\varepsilon_2 = \frac{4[l_{42(\max)}l_{43(\max)} + l_{32}(0)l_{41(\max)}]}{3l_{12}(0)l_{13}(0)\sin\alpha_{213}(0)}\lambda_{\max}(P_2)\sqrt{\frac{V_2(0)}{\lambda_{\min}(P_2)}}$. It follows that if $h_{4-123}(0) > \varepsilon_2$, then agent 4 will never reach the plane formed by agents 1, 2, 3.

Now, we extend the results to the N-agent case by designing the control law for agent $i, 4 \leq i \leq N$ as

$$u_i = \left(\alpha_{ij_1j_2} - \alpha^*_{ij_1j_2}\right)b_{ij_2} + \left(\alpha_{ij_2j_1} - \alpha^*_{ij_2j_1}\right)b_{ij_1} + \left(\alpha_{ij_2j_3} - \alpha^*_{ij_2j_3}\right)b_{ij_3}. \tag{34}$$

Theorem 7: For the N-agent formation under the control (4) and (34), if $\sin\alpha_{jik}(0) \neq 0, j, i, k \in \{1, \ldots, N\}$, the initial angle errors $e_m(0), e_{im}, m = 1, 2, 3$ are sufficiently small, the initial distances $l_{ji}(0)$ are bounded away from zero and $p_i(0)$ is sufficiently away from the plane formed by $p_{j_1}(0), p_{j_2}(0), p_{j_3}(0), j_1, j_2, j_3 \in \mathcal{N}_i$, then the angle errors $e_{im}(t)$ converge exponentially to zero.

The proof of Theorem 7 can be obtained by combining Theorems 4 and 6 and using the reasoning [14, Th. 6].

C. Sequential Formation Control for the Remaining Agents by Type-II Vertex Addition

Now, we investigate the addition of the remaining agents by Type-II vertex addition (we only focus on Case 1, and Case 2 can be similarly analyzed) developed in Definition 8. We design the following control law for agent 4

$$u_4 = -(\alpha_{142} - \alpha^*_{142})(b_{41} + b_{42}) - (\alpha_{243} - \alpha^*_{243})(b_{42} + b_{43}) - (\alpha_{341} - \alpha^*_{341})(b_{43} + b_{41}), \tag{35}$$

where $\alpha^*_{142} \in (0, \pi), \alpha^*_{243} \in (0, \pi), \alpha^*_{341} \in (0, \pi)$ are three desired angles that agent 4 aims at achieving with agents 1, 2, 3. The implementation of (35) only relies on agent 4's direction measurements $\overrightarrow{41}, \overrightarrow{42}, \overrightarrow{43}$, and no interagent communication is required. To obtain the convergence of $\tilde{e}_{41} = \alpha_{142} - \alpha^*_{142}, \tilde{e}_{42} = \alpha_{243} - \alpha^*_{243}, \tilde{e}_{43} = \alpha_{341} - \alpha^*_{341}$, we aim at obtaining the dynamics of $\tilde{e}_{41}, \tilde{e}_{42}, \tilde{e}_{43}$. Since the three components in (35) are similar, we first analyze the dynamics of $\alpha_{i4k}, i, k \in \{1, 2, 3\}$. Using (5) and (35), one has

$$\begin{aligned}\dot{\alpha}_{i4k} &= N_{k4i}\dot{p}_i - (N_{i4k} + N_{k4i})\dot{p}_4 + N_{i4k}\dot{p}_k \\ &= N_{k4i}\dot{p}_i + N_{i4k}\dot{p}_k + e_{4i}\left(N_{i4k}b_{4i} + N_{k4i}b_{4\,k}\right) \\ &\quad + e_{4\,k}\left(N_{k4i}b_{4\,k} + N_{i4k}b_{4\,m} + N_{k4i}b_{4\,m}\right) \\ &\quad + e_{4\,m}\left(N_{i4k}b_{4\,m} + N_{k4i}b_{4\,m} + N_{i4k}b_{4i}\right)\end{aligned} \tag{36}$$

where $N_{kji} = -b^{\mathrm{T}}_{jk}P_{b_{ji}}/(l_{ji}\sin\alpha_{kji}) \in \mathbb{R}^{1\times 3}$ and $m = \{1, 2, 3\}/\{i, k\}$. Defining $f_{ijk} = -N_{ijk}b_{ji} = \sin\alpha_{ijk}/l_{jk} > 0$ and specializing the cases $\{i = 1, k = 2, m = 3\}, \{i = 2, k = 3, m = 1\}, \{i = 3, k = 1, m = 2\}$ in (36) yields the overall angle error dynamics

$$\dot{\tilde{e}}_4 = [\dot{\tilde{e}}_{41}\ \dot{\tilde{e}}_{42}\ \dot{\tilde{e}}_{43}]^{\top} = \tilde{F}_4(e_s, \tilde{e}_4)\tilde{e}_4 + \tilde{G}_4(e_s, \tilde{e}_4)e_s$$

$$= \begin{bmatrix} -f_{142} - f_{241} & h_{(142,3)} - f_{241} & h_{(142,3)} - f_{142} \\ h_{(243,1)} - f_{243} & -f_{243} - f_{342} & h_{(243,1)} - f_{342} \\ h_{(143,2)} - f_{143} & h_{(143,2)} - f_{341} & -f_{341} - f_{143} \end{bmatrix}\begin{bmatrix}\tilde{e}_{41}\\ \tilde{e}_{42}\\ \tilde{e}_{43}\end{bmatrix}$$

$$+ \begin{bmatrix} -N_{241}(b_{12} + b_{13}) & -N_{142}(b_{21} + b_{23}) \\ -N_{342}(b_{21} + b_{23}) & -[N_{243}(b_{31} + b_{32}) \\ & \quad + N_{342}(b_{21} + b_{23})] \\ -N_{341}(b_{31} + b_{32}) & -N_{143}(b_{31} + b_{32}) \\ -N_{143}(b_{31} + b_{32}) & \end{bmatrix}\begin{bmatrix}e_1\\ e_2\end{bmatrix} \tag{37}$$

where $h_{(ijk,m)} = (N_{ijk} + N_{kji})b_{jm}$.

Theorem 8: For the four-agent formation under the control (4) and (35), if

$$0 < h^*_{(i4k,j)} < 2\min\{f^*_{k4i}, f^*_{i4k}\} \tag{38}$$

$i, j, k \in \{1, 2, 3\}, i \neq j \neq k, \sin\alpha_{j4k}(0) \neq 0$, the initial angle errors $\tilde{e}_{4i}(0)$ are sufficiently small, the initial distances $l_{4i}(0)$ are bounded away from zero and $p_4(0)$ is sufficiently away from the plane formed by $p_1(0), p_2(0), p_3(0)$, then the angle errors $\tilde{e}_4(t)$ converge exponentially to zero.

Proof: Linearizing (37) around $\{e_s = 0, e_4 = 0\}$ by following (12), one has the linearized dynamics

$$\dot{\tilde{e}}_4 = \tilde{A}_4\tilde{e}_4 + \tilde{B}_4e_s \tag{39}$$

where $\tilde{A}_4 = \tilde{F}_4(e_s, \tilde{e}_4)|_{e_s=0,\tilde{e}_4=0}$, $B_4 = G_4(e_s, e_4)|_{e_s=0,e_4=0}$. To obtain the stability of the linearized system (39), we aim at proving that $\tilde{A}_4$ is Hurwitz. By using the Gershgorin circle theorem [41, Th. 6.1.1], the three eigenvalues of $\tilde{A}_4$ must lie within the union of the following three Gershgorin discs

$$|\lambda + f^*_{i4j} + f^*_{j4i}| \leq |h^*_{(i4j,k)} - f^*_{i4j}| + |h^*_{(i4j,k)} - f^*_{j4i}| \tag{40}$$

where $i,j,k\in\{1,2,3\}, i\neq j\neq k$. Note that $f^*_{i4k}>0$ for all $i,k=1,2,3$. Therefore, by using (38), one has

$$0<|h^*_{(j4i,k)}-f^*_{i4j}|+|h^*_{(i4j,k)}-f^*_{j4i}|<f^*_{i4j}+f^*_{j4i}. \quad (41)$$

By combining (40) with (41), one has that the union of the three Gershgorin discs in (40) always lies in the left half of the complex plane, which implies that the three eigenvalues of $\tilde{A}_4$ have negative real parts. Therefore, (38) is a sufficient condition to guarantee that matrix $\tilde{A}_4$ is Hurwitz which implies the exponential convergence of $\tilde{e}_4$ by following (28)–(30).

Also following (31)–(33), one can precisely describe the requirements on $l_{ji}(0)$, $\tilde{e}_{4i}(0)$ and the initial distance $h_{4-123}(0)$ in this case. Similarly, we can extend the results to N-agent case by designing the following control law:

$$u_i=-\left(\alpha_{j_1ij_2}-\alpha^*_{j_1ij_2}\right)\left(b_{ij_1}+b_{ij_2}\right)-\left(\alpha_{j_2ij_3}-\alpha^*_{j_2ij_3}\right)\left(b_{ij_2}+b_{ij_3}\right)-\left(\alpha_{j_3ij_1}-\alpha^*_{j_3ij_1}\right)\left(b_{ij_3}+b_{ij_1}\right),\ 4\le i\le N \quad (42)$$

where $\alpha^*_{j_1ij_2}\in(0,\pi), \alpha^*_{j_2ij_3}\in(0,\pi), \alpha^*_{j_3ij_1}\in(0,\pi)$. Then, the convergence result can be obtained following Theorem 7.

Remark 7: To implement the proposed sequential formation laws, each agent is allowed to have its own local coordinate frame [14]. Compared with the control law (42), which only needs local direction measurements, the control law (34) needs not only direction measurements, but also interagent communication. However, (42) can only stabilize tetrahedral formation satisfying (38), and (34) can stabilize an arbitrary tetrahedral formation, which is also an advantage over the 2-D control laws [14]. In addition, the 3-D control laws proposed in Sections IV-A and IV-B are based on pursuing rule, which is different from the bisector rule proposed in 2-D case [14].

D. Convex Polyhedral Formations

Different from the sequential formations, we assume that the angle constraints are only in the faces of a convex polyhedral formation. From Theorem 2, we first show how to stabilize a convex polyhedral angle rigid formation with 4 triangular faces and 12 angle constraints, then extend it to more general cases. The control laws for the four agents are designed as

$$u_i=-e_{jik}b_{ik}-e_{mij}b_{ij}-e_{kim}b_{im} \quad (43)$$

where $i\neq j\neq k\neq m$, $i,j,k,m\in\{1,2,3,4\}$, $e_{ijk}=\alpha_{ijk}-\alpha^*_{ijk}$. Using the calculations (36), one has the error dynamics

$$\begin{aligned}\dot{e}_{ijk}&=N_{ijk}\left(\dot{p}_k-\dot{p}_j\right)+N_{kji}\left(\dot{p}_i-\dot{p}_j\right)\\&=N_{ijk}\left(-e_{ikm}b_{km}-e_{jki}b_{ki}+e_{ijm}b_{jm}+e_{kji}b_{ji}\right)\\&\quad+N_{kji}\left(-e_{jik}b_{ik}-e_{kim}b_{im}+e_{ijm}b_{jm}+e_{mjk}b_{jk}\right).\end{aligned} \quad (44)$$

By specifying all possible combinations of i,j,k,m for (44), one will have the error dynamics of the 12 face angles. However, the three angles in each face of the tetrahedron are linearly dependent, e.g., $e_{123}+e_{231}+e_{312}=0$. Therefore, we choose in each face two interior angles to form the state variable $e_s=[e_{123},e_{231},e_{234},e_{243},e_{214},e_{241},e_{341},e_{314}]^\top$ and take $\mathcal{A}_1=\{(1,2,3),(2,3,1),(2,3,4),(2,4,3),(2,1,4),(2,4,1),(3,4,1),(3,1,4)\}$. Then, one has the closed-loop angle error dynamics

$$\dot{e}_s=A(e_s)e_s \quad (45)$$

where $A(e_s)\in\mathbb{R}^{8\times8}$ consists of the coefficients of the angle errors in (44). Following the linearization step, (45) can be linearized as $\dot{e}_s=A^*_se_s$ where $A^*_s=A(e_s)|_{e_s=0}$.

Theorem 9: For the four-agent convex polyhedral formation under the control (43), if

$$\begin{aligned}\frac{\sin\alpha^*_{ijk}+\sin\alpha^*_{jki}}{l^*_{jk}}&>\left|\frac{\sin\alpha^*_{kij}}{l^*_{ji}}-\frac{\sin\alpha_{jki}}{l^*_{jk}}\right|+|N^*_{ijk}b^*_{km}|\\&\quad+|N^*_{ijk}b^*_{jm}|+|N^*_{kji}b^*_{im}|+|N^*_{kji}b^*_{jm}|+|N^*_{kji}b^*_{jk}|\end{aligned} \quad (46)$$

where $(i,j,k)\in\mathcal{A}_1$, $m=\{1,2,3,4\}/\{i,j,k\}$, $\sin\alpha_{ijk}(0)\neq0$, the initial angle errors $e_{ijk}(0)$ are sufficiently small, and the initial distances $l_{ij}(0)$ are bounded away from zero, then the angle errors $e_{ijk}(t)$ converge exponentially to zero.

Proof: To check the local stability of (45), we examine the eigenvalue distribution of matrix $A^*_s\in\mathbb{R}^{8\times8}$. Taking e_{423} as an example, its linearized dynamics can be written as

$$\begin{aligned}\dot{e}_{423}=&-\frac{\sin\alpha^*_{423}+\sin\alpha^*_{234}}{l^*_{23}}e_{423}+\left[\frac{\sin\alpha^*_{342}}{l^*_{24}}-\frac{\sin\alpha^*_{234}}{l^*_{23}}\right]e_{243}\\&-N^*_{423}b^*_{31}e_{431}+N^*_{423}b^*_{21}e_{421}-N^*_{324}b^*_{41}e_{341}\\&+N^*_{324}b^*_{21}e_{421}+N^*_{324}b^*_{23}e_{123}\end{aligned} \quad (47)$$

Using [41, Th. 6.1.1] again, to render the eigenvalue to be in the left half of the complex plane, one requires

$$\begin{aligned}&(\sin\alpha^*_{423}+\sin\alpha^*_{234})/l^*_{23}>|\sin\alpha^*_{342}/l^*_{24}-\sin\alpha^*_{234}/l^*_{23}|\\&+|N^*_{423}b^*_{31}|+|N^*_{423}b^*_{21}|+|N^*_{324}b^*_{41}|+|N^*_{324}b^*_{21}|+|N^*_{324}b^*_{23}|\end{aligned}$$

which is one case of (46). Using the same step for the other angles, the similar condition can be obtained. Thus, if the condition (46) holds for all the six angles defined in $\mathcal{A}_1$, then A^*_s is Hurwitz, which implies the local stability of (45).

For an N-agent convex polyhedral formation, the control law for agent $i, 1\le i\le N$ can be designed as $u_i=-\sum_{(j,i,k)\in\mathcal{A}}e_{jik}b_{ik}$, where $\mathcal{A}$ is the angle set containing all the angles of the triangular faces of the convex polyhedral formation. Using similar steps as (44)–(47), a stability condition can be obtained to guarantee the local stability of the convex polyhedral formation with triangular faces.

Remark 8: For all the designed formation control laws in this section, the measurement topology is described by the desired angle constraints, i.e., if there is an α^*_{ijk}, then agent j needs to measure $\overrightarrow{ji},\overrightarrow{jk}$. While the communication topology only appears in (34), where if there is an $\alpha^*_{ij_1j_2}, j_1<i, j_2<i$, then agent j_1 needs to send the measured $\alpha_{ij_1j_2}$ to agent i. Note that both the measurement and communication topology are distributed. In addition, the checking conditions (38) and (46) can be transformed to be related only with desired angles by using the law of sines.

Remark 9: Since the designed direction-only formation control laws are for single-integrators, to apply them to real robotic vehicles, such as quadrotors, the feedforward of the vehicles' nonlinear dynamics and feedback of the vehicles' velocity are usually needed [42]. Another important aspect is the on-board sensing of the intervehicle directions, which can be accessed by

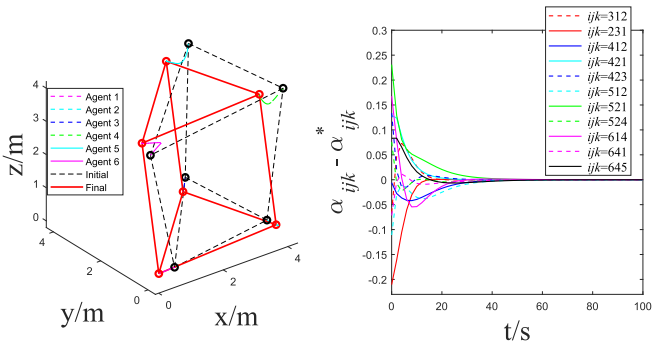

Fig. 10. Formation trajectories and evolution of angle errors under the controller (4) and (20).

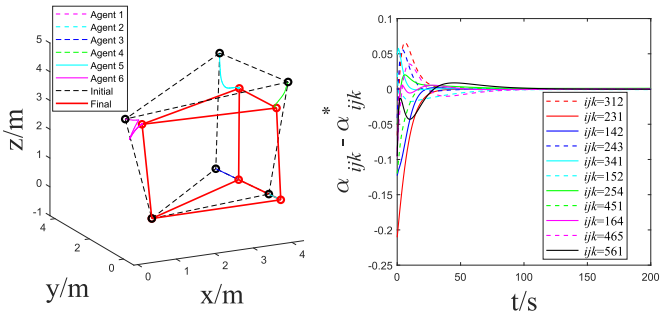

Fig. 11. Formation trajectories and evolution of angle errors under the controller (15) and (35).

monocular cameras with tag recognition, direction finding-based Bluetooth 5.1 modules, and AOA-based UWB modules. We also remark that direction-only formation control laws will be useful for those coordinated tasks where the intervehicle distances are hard to be measured, e.g., for swarm satellites and autonomous underwater vehicles (AUV).

V. Simulation Examples

In this section, we use numerical examples with six agents forming a triangular prism to validate the effectiveness of the proposed formation control laws. The desired formation is constructed by starting from $\triangle 123$ and adding the remaining agents 4–6 sequentially through Type-I or Type-II vertex additions. The tetrahedra used for vertex additions are $\triangle 4123$, $\triangle 5124$, $\triangle 6145$. We initialize all agents' positions as $p_1(0) = [0.5, -0.3, 0.4]^\top$, $p_2(0) = [3.8, 0.3, 0.4]^\top$, $p_3(0) = [4.2, 4.3, -0.2]^\top$, $p_4(0) = [4.3, 0.3, 4.2]^\top$, $p_5(0) = [4.3, 4.3, 3.8]^\top$, $p_6(0) = [-0.1, -0.1, 3.9]^\top$. The desired angles are $\alpha^*_{123} = \pi/2, \alpha^*_{231} = \pi/4, \alpha^*_{412} = \pi/4, \alpha^*_{421} = \pi/2, \alpha^*_{423} = \pi/2, \alpha^*_{512} = \arccos(\sqrt{2}/4), \alpha^*_{521} = \pi/2, \alpha^*_{524} = \pi/4, \alpha^*_{614} = \pi/4, \alpha^*_{641} = \pi/4, \alpha^*_{645} = \pi/2$.

When the six-agent formation is controlled by (4) and (20), i.e., constructed by Type-I vertex addition, Fig. 10 gives the formation trajectories and the evolution of angle errors. When the six-agent formation is controlled by (15) and (35), i.e., constructed by Type-II vertex addition, Fig. 11 gives the formation trajectories and the evolution of angle errors. Also, we simulate the case where each agent i's single-integrator model is added by disturbances $0.01 * [\sin(it), \sin(it + \pi/2), \sin(it + \pi)]^\top, i = 1, \ldots, 6$. Fig. 12 gives the formation trajectories and the evolution of angle errors under the control laws (4) and (20) and disturbances.

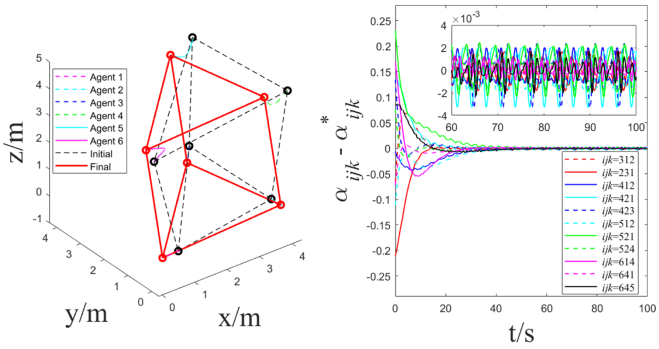

Fig. 12. Formation trajectories and evolution of angle errors under the controller (15), (35) and disturbances.

The achievement of the desired triangular prism formation and the convergence of the angle errors in Figs. 10–12 illustrate the effectiveness of the proposed formation control laws. For the evolution of angle errors in Figs. 10 and 11, the convergence speed of the angle errors in Fig. 10 is faster. From Fig. 11, $|\alpha_{231} - \alpha^*_{231}|$ decreases monotonically and agents 2 and 3 move along the line formed by $p_2(0)$ and $p_3(0)$, which validate the result of Theorem 5. In Fig. 12, the angle errors after convergence are within 5×10^{-3}, which illustrates the formation's robustness against disturbances.

VI. Conclusion

In this article, we have proposed 3-D angle rigidity theory and applied it to multiagent direction-only formation control. First, by constructing an angle rigid angularity with flex ambiguity, we have shown that angle rigidity in 3-D is a local property. To construct globally angle rigid and angle rigid angularities, two types of vertex addition operations have been developed, respectively. Motivated by Laman theorem, minimal angle rigidity has been investigated. When angle constraints are given in surfaces of polyhedra, angle rigidity of convex polyhedra has been studied by employing properties of perturbations for rigid frameworks. Using the developed 3-D angle rigidity, we have designed 3-D direction-only formation laws by following those two types of construction approaches and the intuition of angle error feedback.

This article has investigated 3-D angle rigidity and applied it to direction-only multiagent formations. Our future work on angle rigidity will consider the extension of 3-D angle rigidity to higher dimensional spaces, and the necessary and sufficient condition for angle rigidity. Our future work on formation control will focus on direction-only multiagent formations governed by more complicated agent dynamics, such as quadrotor dynamics, AUV dynamics, spacecraft dynamics, and high-order dynamics.

References

[1] L. Euler, "Opera postuma," *Euler Arch. Index Number E819*, vol. 1, pp. 494–496, 1862.
[2] A. L. Cauchy, "Sur les polygones et les polyedres, seconde mémoire," *J. Ecole Polytechnique*, vol. 16, no. 9, pp. 26–38, 1813.

[3] B. D. Anderson, C. Yu, B. Fidan, and J. M. Hendrickx, "Rigid graph control architectures for autonomous formations," *IEEE Control Syst. Mag.*, vol. 28, no. 6, pp. 48–63, Dec. 2008.
[4] M. D. Collins, M. L. Quillin, G. Hummer, B. W. Matthews, and S. M. Gruner, "Structural rigidity of a large cavity-containing protein revealed by high-pressure crystallography," *J. Mol. Biol.*, vol. 367, no. 3, pp. 752–763, 2007.
[5] D. Bi, J. Lopez, J. M. Schwarz, and M. L. Manning, "A density-independent rigidity transition in biological tissues," *Nature Phys.*, vol. 11, no. 12, pp. 1074–1079, 2015.
[6] L. Asimow and B. Roth, "The rigidity of graphs," *Trans. Amer. Math. Soc.*, vol. 245, pp. 279–289, 1978.
[7] R. Connelly, "Generic global rigidity," *Discrete Comput. Geometry*, vol. 33, no. 4, pp. 549–563, 2005.
[8] B. Jackson and T. Jordán, "Connected rigidity matroids and unique realizations of graphs," *J. Combinatorial Theory, Ser. B*, vol. 94, no. 1, pp. 1–29, 2005.
[9] R. Connelly, "On generic global rigidity, applied geometry and discrete mathematics," *DIMACS Ser. Discrete Math. Theoret. Comput. Sci*, vol. 4, pp. 147–155, 1991.
[10] S. Zhao and D. Zelazo, "Bearing rigidity and almost global bearing-only formation stabilization," *IEEE Trans. Autom. Control*, vol. 61, no. 5, pp. 1255–1268, May 2016.
[11] G. Michieletto, A. Cenedese, and D. Zelazo, "A unified dissertation on bearing rigidity theory," *IEEE Trans. Control Netw. Syst.*, vol. 8, no. 4, pp. 1624–1636, Dec. 2021.
[12] D. Zelazo, P. R. Giordano, and A. Franchi, "Bearing-only formation control using an SE (2) rigidity theory," in *Proc. IEEE 54th Conf. Decis. Control*, 2015, pp. 6121–6126.
[13] G. Jing, G. Zhang, H. W. J. Lee, and L. Wang, "Angle-based shape determination theory of planar graphs with application to formation stabilization," *Automatica*, vol. 105, pp. 117–129, 2019.
[14] L. Chen, M. Cao, and C. Li, "Angle rigidity and its usage to stabilize multi-agent formations in 2D," *IEEE Trans. Autom. Control*, vol. 66, no. 8, pp. 3667–3681, Aug. 2021.
[15] I. Buckley and M. Egerstedt, "Infinitesimal shape-similarity for characterization and control of bearing-only multirobot formations," *IEEE Trans. Robot.*, vol. 37, no. 6, pp. 1921–1935, Dec. 2021.
[16] H.-S. Ahn, *Formation Control*. Berlin, Germany: Springer, 2020.
[17] H. G. De Marina, B. Jayawardhana, and M. Cao, "Distributed rotational and translational maneuvering of rigid formations and their applications," *IEEE Trans. Robot.*, vol. 32, no. 3, pp. 684–697, Jun. 2016.
[18] K. Sakurama, "Unified formulation of multi-agent coordination with relative measurements," *IEEE Trans. Autom. Control*, vol. 66, no. 9, pp. 4101–4116, Sep. 2021.
[19] L. Krick, M. E. Broucke, and B. A. Francis, "Stabilisation of infinitesimally rigid formations of multi-robot networks," *Int. J. Control*, vol. 82, no. 3, pp. 423–439, 2009.
[20] R. Olfati-Saber and R. M. Murray, "Graph rigidity and distributed formation stabilization of multi-vehicle systems," in *Proc. IEEE 41st Conf. Decis. Control*, 2002, vol. 3, pp. 2965–2971.
[21] Z. Sun, B. D. Anderson, M. Deghat, and H.-S. Ahn, "Rigid formation control of double-integrator systems," *Int. J. Control*, vol. 90, no. 7, pp. 1403–1419, 2017.
[22] S. Zhao and D. Zelazo, "Bearing rigidity theory and its applications for control and estimation of network systems: Life beyond distance rigidity," *IEEE Control Syst. Mag.*, vol. 39, no. 2, pp. 66–83, Apr. 2019.
[23] M. Basiri, A. N. Bishop, and P. Jensfelt, "Distributed control of triangular formations with angle-only constraints," *Syst. Control Lett.*, vol. 59, no. 2, pp. 147–154, 2010.
[24] S.-H. Kwon and H.-S. Ahn, "Generalized weak rigidity: Theory, and local and global convergence of formations," *Syst. Control Lett.*, vol. 146, 2020, Art. no. 104800.
[25] H. Gluck, "Almost all simply connected closed surfaces are rigid," in *Geometric Topology*. Berlin, Germany: Springer, 1975, pp. 225–239.
[26] G. Michieletto and A. Cenedese, "Formation control for fully actuated systems: A quaternion-based bearing rigidity approach," in *Proc. IEEE 18th Eur. Control Conf.*, 2019, pp. 107–112.
[27] F. Schiano, A. Franchi, D. Zelazo, and P. R. Giordano, "A rigidity-based decentralized bearing formation controller for groups of quadrotor UAVs," in *Proc. IEEE/RSJ Int. Conf. Intell. Robots Syst.*, 2016, pp. 5099–5106.
[28] T. Eren, "Formation shape control based on bearing rigidity," *Int. J. Control*, vol. 85, no. 9, pp. 1361–1379, 2012.
[29] R. Connelly, "Rigidity," in *Handbook of Convex Geometry*. Amsterdam, The Netherlands: Elsevier, 1993, pp. 223–271.
[30] B. D. Anderson, Z. Sun, T. Sugie, S.-I. Azuma, and K. Sakurama, "Formation shape control with distance and area constraints," *IFAC J. Syst. Control*, vol. 1, pp. 2–12, 2017.
[31] T. Liu and M. de Queiroz, "An orthogonal basis approach to formation shape control," *Automatica*, vol. 129, 2021, Art. no. 109619.
[32] A. D. Alexandrov, *Convex Polyhedra*. Berlin, Germany: Springer, 2005.
[33] X. Li, Y. Bai, X. Dong, Q. Li, and Z. Ren, "Distributed time-varying formation control with uncertainties based on an event-triggered mechanism," *Sci. China Inf. Sci.*, vol. 64, no. 3, pp. 1–10, 2021.
[34] M. H. Trinh, S. Zhao, Z. Sun, D. Zelazo, B. D. Anderson, and H.-S. Ahn, "Bearing-based formation control of a group of agents with leader-first follower structure," *IEEE Trans. Autom. Control*, vol. 64, no. 2, pp. 598–613, Feb. 2019.
[35] X. Chai, J. Liu, Y. Yu, and C. Sun, "Observer-based self-triggered control for time-varying formation of multi-agent systems," *Sci. China Inf. Sci.s*, vol. 64, no. 3, pp. 1–16, 2021.
[36] I. Buckley and M. Egerstedt, "Controller synthesis for infinitesimally shape-similar formations," in *Proc. IEEE Int. Conf. Robot. Automat.*, 2020, pp. 5597–5603.
[37] M. Cao, A. S. Morse, C. Yu, B. D. Anderson, and S. Dasguvta, "Controlling a triangular formation of mobile autonomous agents," in *Proc. IEEE 46th Conf. Decis. Control*, 2007, pp. 3603–3608.
[38] I. Buckley and M. Egerstedt, "Infinitesimally shape-similar motions using relative angle measurements," in *Proc. IEEE/RSJ Int. Conf. Intell. Robots Syst.*, 2017, pp. 1077–1082.
[39] A. N. Bishop, "A very relaxed control law for bearing-only triangular formation control," *IFAC Proc. Volumes*, vol. 44, no. 1, pp. 5991–5998, 2011.
[40] S. Sastry and M. Bodson, *Adaptive Control: Stability, Convergence and Robustness*. Chelmsford, MA, USA: Courier Corporation, 2011.
[41] R. A. Horn and C. R. Johnson, *Matrix Analysis*. Cambridge, U.K: Cambridge Univ. Press, 2012.
[42] C. Deng, C. Wen, W. Wang, X. Li, and D. Yue, "Distributed adaptive tracking control for high-order nonlinear multi-agent systems over event-triggered communication," *IEEE Trans. Autom. Control*, to be published, doi: 10.1109/TAC.2022.3148384.

Liangming Chen received the B. E. degree in automation from Southwest Jiaotong University, Chengdu, China, in 2015.

He is currently an Associate Professor with Southern University of Science and Technology, Shenzhen, China. From 2015 to 2021, he was enrolled jointly in the Ph.D. programs of systems and control with the Harbin Institute of Technology, China, and the University of Groningen, the Netherlands. From 2021 to 2022, he was a Research Fellow with Nanyang Techonological University, Singapore. His research interests are in rigidity theory and multi-agent systems.

Ming Cao (Fellow, IEEE) received the bachelor's degree in 1999 and the master's degree in 2002 from Tsinghua University, China, and the Ph.D. degree in 2007 from Yale University, New Haven, CT, USA, all in electrical engineering.

He is currently a Professor of systems and control with the Engineering and Technology Institute (ENTEG), the University of Groningen, Groningen, the Netherlands, where he started as an Assistant Professor in 2008. From 2007 to 2008, he was a Postdoctoral Research Associate with the Department of Mechanical and Aerospace Engineering, Princeton University, Princeton, NJ, USA. He worked as a Research Intern in 2006 with the Mathematical Sciences Department, IBM T. J. Watson Research Center, USA. His main research interest is in autonomous agents and multi-agent systems, decision making dynamics and complex networks.

Dr. Cao is the 2017 and inaugural recipient of the Manfred Thoma medal from the International Federation of Automatic Control (IFAC) and the 2016 recipient of the European Control Award sponsored by the European Control Association (EUCA). He is a Senior Editor for SYSTEMS AND CONTROL LETTERS, an Associate Editor for IEEE TRANSACTIONS ON AUTOMATIC CONTROL, IEEE TRANSACTIONS ON CIRCUITS AND SYSTEMS and IEEE CIRCUITS AND SYSTEMS MAGAZINE